UNIVERSIDAD AUTÓNOMA DE NUEVO LEÓN

FACULTAD DE CIENCIAS FÍSICO MATEMÁTICAS

TESIS

A DISTRIBUTION-FREE SHEWHART-TYPE LEPAGE CONTROL CHART FOR JOINT MONITORING OF LOCATION AND SCALE IN FINITE HORIZON PRODUCTIONS

Presentada por:

ARTURO JAVIER DÍAZ PULIDO

Para optar por el grado de

MAESTRÍA EN CIENCIAS

CON ORIENTACIÓN EN MATEMÁTICAS

2021

Universidad Autónoma de Nuevo León

Facultad de Ciencias Físico Matemáticas

Centro de Investigación en Ciencias Físico Matemáticas

tesis

A distribution-free Shewhart-type Lepage control chart for joint monitoring of location and scale in finite horizon productions

por

Arturo Javier Díaz Pulido

en opción al grado de

Maestría en Ciencias

con Orientación en Matemáticas

San Nicolás de los Garza, Nuevo León, México Fecha

Contents

Chapter 1

Introduction

Abstract

Finite horizon production (FHP) processes are common in manufacturing environments characterized by a high degree of flexibility, production variety, and a limited number of scheduled inspections. Due to its characteristics, research on statistical tools for monitoring FHP processes has increased in recent years. Because of the constant changes in the production process, the distribution of the quality characteristic is often unknown, and online monitoring is needed as fast as possible, having no time for a Phase I SPC analysis. Celano and Chakraborti Celano and Chakraborti, 2020 implemented a distribution-free Shewhart-type Mann-Whitney control chart for monitoring location in FHP processes; where they evaluated the conditional performance of the control chart selecting the control limits following an 'exceedance probability criterion' (EPC), see Jardim et al., 2020, guaranteeing a desired in-control performance of the control chart in terms of false alarm probability (FAP). In this research, we propose a Shewhart control chart for monitoring location and scale on an FHP process using a Lepage-type statistic composed by the combination of the Wilcoxon and Mood statistics. The control limits were selected under the conditional perspective, taking into account the practitioner to practitioner variability. We performed a Monte-Carlo simulation study to evaluate the performance of the proposed chart. Results show that the proposed control chart is effective to detect medium and larges changes in location or scale, whereas it preserves a desirable in-control performance.

1.0.1 Motivation

Statistical process control (SPC) is the use of statistical tools and procedures that help practitioners monitor process behavior, discover issues in internal systems, and find solutions for production issues. In SPC, various aspects within a process are monitored and controlled to maintain full potential during the manufacturing processes. Zhang, 2010 says " Statistical Process Control (SPC) is a control method for monitoring an industrial process through the use of a control chart. Much of its power lies in its ability to monitor both the process center and its variation about that center." (p.41). Kiran, 2017, wrote about SPC, "determines the stability and predictability of a process. It can be

applied to any process where the output of the product conforming to specifications can be measured."

In the early 1920s, Walter Shewhart of Bell Laboratories pioneered the concept of SPC by developing a statistical tool for monitoring a process named control chart. In 1931, Shewhart authored a book entitled Economic Control of Quality of Manufactured Product which settled the stage for the statistical use within processes to improve product control. Some years after that, the professional society was formed in 1945 regarding SPC - The American Society for Quality Control. During this restraint of time, SPC methods were introduced to the Japanese industry as well.

Control charts are one of the most important statistical tools in the SPC, used to establish the state of statistic control in either a business or fabrication process. The primary objective of a control chart is to continuously register data so discrepancies or anomalous events can be observed within the typical process performance. There are two different types of process variation: Common cause variation and special cause variation.

- **Common Cause Variation :** This variation can be considered natural or common to the process and will nearly always be present. If only this variation is detected in the process, then this process is considered in control.

- **Special Cause Variation:** This variation can be explained by an external factor, increasing the total variation of the process. When special causes are detected, we say that the process is out of control.

The application of SPC involves two main phases; in Phase I, the process is stabilized, and the special causes of variation are eliminated; when there are no special causes of variation in the Phase I sample, the sample is In Control (IC). In Phase II, the process is monitored using statistics of the ongoing samples, which are evaluated according to the IC sample looking for changes in location or scale. In SPC, the distribution of the IC variable is often assumed as known. The most popular assumption in the literature is that the probability distribution under analysis is normal; moreover, the underlying process is not normal in many applications. As a result, the statistical properties of the standard control charts can be highly affected. Another relevant assumption is that the processes run for an infinite time until a change occurs. There are ample justifications for developing and applying control charts with properties that do not depend on normal-

ity or any other specific distributional assumption. Distribution-free and non-parametric control charts are designed to achieve this purpose.

In industry, there exist processes in which the number of scheduled inspections before it ends should be restricted to a few tens. These processes are known as finite horizon production processes (FHP). In many industrial fields, the processes should be frequently reconfigured to respond promptly to the market demand of different products. They are present in the baby diaper companies, mechanical and electronic industries, food production of multi-branded products, among others.
There are essential issues that practitioners face when they want to use the SPC tools to monitor these type of processes, like:

- After each process set-up and restart following a production switch to a new part code, the current distribution of the quality characteristic is unknown.
- The control chart's performance should be measured by metrics accounting for the small number of inspections during the production run.

Recently, Celano and Chakraborti, 2020 implemented a distribution-free Shewhart-type Mann-Whitney control chart for monitoring finite horizon productions for the unknown parameter case and with a reference sample scheme. They evaluate the statistical performance of the control chart, conditional on the selected reference sample. This thesis proposes a new control chart for joint monitoring the location and scale of a finite horizon production using a Lepage-type statistic, evaluating the conditional statistical performance in a reference sample scheme.

1.0.2 Problem statement and context

A new control chart for joint monitoring the location and scale parameters in an FHP process based on a Lepage-Mood statistic is proposed in this research, with a "guaranteed performance." This investigation was done by looking for control limits that guarantee the desired performance for a high percentage of the practitioners, named the conditional scheme. Monte Carlo simulation is used to evaluate the performance of this Lepage-type control chart. The in-control performance of the proposed chart is compared with the same chart under the unconditional approach, whereas the out-of-control performance is evaluated with the proposed control chart and the one using the Lepage statistic formed by Wilcoxon and Ansari-Bradley statistics.

1.0.3 Research questions

1. Is the proposed control chart based on the Lepage-Mood statistic effective for monitoring the location and scale parameters in a finite horizon production process?.

2. Is the proposed control chart under the conditional perspective a better alternative in terms of the in-Control performance than the control chart based on the unconditional perspective?.

3. Is the proposed control chart based on the Lepage-Mood statistic more potent in terms of Out-of-control performance with the conditional scheme than the alternative of using the Lepage-Ansari-Bradley statistic?

1.0.4 Hypotheses

1. The proposed control chart based on the Lepage-Mood statistic is effective (considering effectiveness as showing a low false alarm probability and power for detecting true alarms).

2. Under the conditional perspective, the proposed control chart is a better alternative in terms of In-Control performance than the control chart based on the unconditional perspective.

3. The proposed control chart is more potent in terms of Out-of-control performance with the conditional scheme than using the common Lepage-Ansari-Bradley statistic.

1.0.5 Objectives

The main goal of this research is to propose an effective control chart for joint monitoring the location and scale parameters in a finite horizon production process when the distributions of the observations are unknown, with guaranteed In-control performance.

The primary objective can be divided into specific targets to address the hypotheses mentioned in Section 1.4:

1. Look at the effectiveness in terms of a low and controlled false alarm probability of the control chart through a simulation study to evaluate the statistical performance of the control chart.

2. Measure the In-control statistical performance (in terms of conditional False Alarm Probability) of the proposed control chart based on the Lepage-Mood statistic and compare both the conditional and unconditional perspectives.

3. Measure the Out-of-control statistical performance of the proposed control chart (in terms of conditional Signal Probability) of the proposed control chart based on the Lepage-Mood statistic and compare it with the Lepage-Ansari-Bradley statistic.

1.0.6 Scope and Limitations

In this thesis, the scope is to create and evaluate a control chart for finite horizon production processes (FHP) that monitors the location and scale parameters of the process.

The study covers the use of the Lepage-Mood statistic used in Tercero-Gómez et al., 2020 and classical Lepage statistic (only for comparison purposes in the Out-of-control performance section) for monitoring changes in the location and scale parameters under a variety of scenarios.

The covered scenarios in which the study is limited are:

- Using only two-sample tests, Mood and AB.
- A fix target False Alarm Probability (FAP_0) equal to 0.1
- Sample size. Reference sample sizes are 20, 30, 40, 50, 60, 70, 80, 90, 100, 150, 200, 350 and 500 and test sample size can be 5, 10 and 25.
- Distribution. The performance of the control chart is evaluated for two symmetric distributions, $N(0, 1)$ and $t(4)$ and two asymmetric distributions, $Gamma(2, 1)$ and $Gamma(3, 1)$.
- Change size. Combinations are considered for changes in location (0, 0.25, 0.5, 0.75, 1, 1.5, 2), scale (0.25, 0.5, 0.66, 1, 1.5, 2, 3) or both of them at the same time measured in standard deviations.
- The number of replicates using the Monte Carlo simulations is fixed to 10,000.

Chapter 2

Background and Literature Review

2.1 Control Charts

A control chart is a statistical tool used to study how a process changes over time, in which statistics of the monitored samples are obtained and evaluated in order to determine if the process is in-control or not. A traditional control chart has a central line for the statistic monitored, an upper control limit, and a lower control limit. These control limits are established from historical data, the distribution of the statistic observed, or assumptions over the data distribution. By comparing recent data to these limits, you can conclude whether the process variation is consistent (in control) or unreliable (out of control, affected by special causes of variation).

Traditional control charts are mainly designed to monitor process parameters when the underlying distribution of the process is known. However, there are a lot of practical applications where the distribution of the process is unknown, making the distribution-free control charts a best option for practitioners.

A charting statistic defined by the observed data should be selected. It must contain as much of the information in the empirical data about the distribution of the quality characteristic(s) as possible and be susceptible to any shift. The most common control charts are the Shewhart type control charts, CUSUM type control charts, the exponentially weighted moving average (EWMA) control charts, and the control charts based on change-point detection (CPD).

The first control chart in the literature was proposed in Shewhart, 1926, and is called the Shewhart chart. Over the past 80 years, many different versions of the Shewhart chart

have been proposed for different purposes, and they are widely used in practice. But, the disadvantage of the Shewhart chart is the lack of sensitiveness to detect small to moderate shifts in the process. As an example of the Shewhart-type control charts, lets explain the Shewhart $\bar{X}$ control chart, where we assume that the IC mean μ_0 and standard deviation σ_0 of the quality characteristic are both known. Then, at each monitoring time point t we collect a sample of n observations $x_1, x_2, \ldots, x_n$ and compute its average

$$\bar{x} = \frac{x_1 + x_2 + \ldots + x_n}{n} \tag{2.1}$$

and we know that, $\bar{x} \sim N(\mu_0, \frac{\sigma_0}{n})$. Thus, when we want to monitor a shift in the mean of the process, it is natural to consider the following hypothesis testing:

$$H_0: \quad \mu = \mu_0 \quad vs \quad H_1: \quad \mu \neq \mu_0$$

where μ denotes the true mean of the process. With this, we generate the upper and lower control limits for the control chart as

$$UCL = \mu_0 + k\frac{\sigma_0}{\sqrt{n}} \tag{2.2}$$

$$LCL = \mu_0 - k\frac{\sigma_0}{\sqrt{n}} \tag{2.3}$$

where k is the control limit coefficient, typically SPC practitioners have considered $k = 3$, so the three-sigma limits are employed. Therefore the interval $[UCL, LCL]$ covers approximately 99.73% of the population. In practice, the values of μ_0 and σ_0 are unknown, and we need to estimate them from a Phase I sample. For more details see Qiu, 2014. Figure 2.1 shows an example of the implementation of a Shewhart $\bar{X}$ control chart. The data used in this example is from table 6E.11 in Montgomery, 2009. The control chart is constructed for an injection molding process example with 20 samples, each one of size 5.

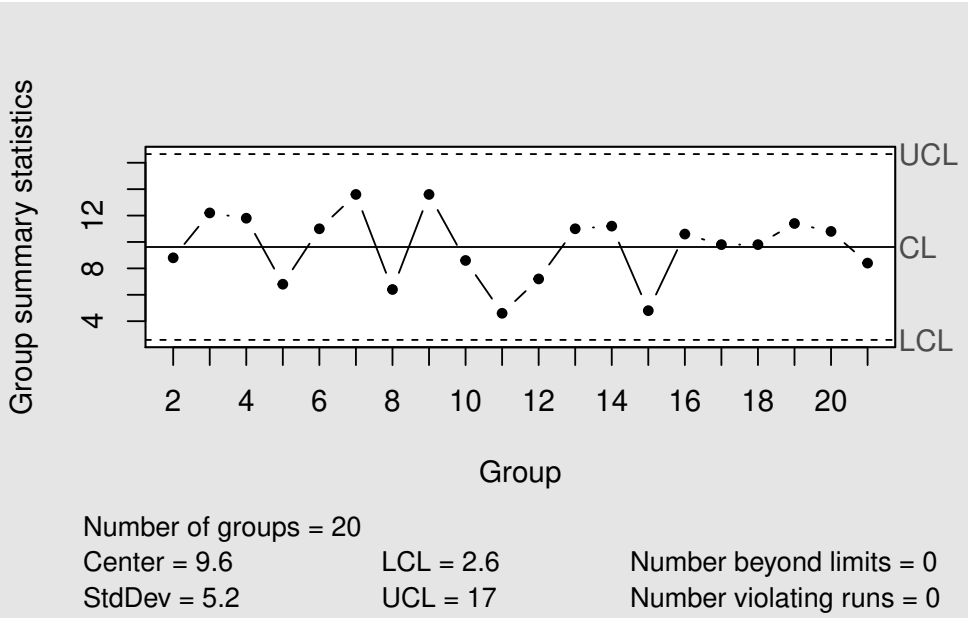

Figure 2.1: Shewhart $\bar{X}$ control chart example for monitoring an injection molding process

Another control chart coomonly used is the Cumulative Sum control chart CUSUM, proposed in Page, 1954. This control chart is an efficient alternative to overcome the problem of detecting small to moderate shifts in the process. The statistic used in this control chart is the cumulative sum of deviations from a target. This control chart requires two parameters, k the reference value, k is usually set to half the shift to be detected, in sigma units, and h, the decision limit specified in sigma units. In the typical model for a CUSUM chart, we assume that the IC distribution of the quality characteristic to be monitored is $N(\mu_0, \sigma^2)$ and we are looking for potential shift in in the mean of the production process. Assume that $X_1, X_2, \ldots$ are individual observation data obtained online at consecutive time points from a production process. The observations are independent and identically distributed (i.i.d.) with a common IC distribution $N(\mu_0, \sigma^2)$ before a process mean shift. With this settings, we considered the charting statistic

$$C_t = \sum_{i=1}^{t} (X_i - \mu_0) \tag{2.4}$$

where $C_0 = 0$. It is obvious that $C_t = C_{t-1} + (X_t - \mu_0)$, therefore, C_t is a cumulative sum of the deviations $\{X_i - \mu_0, i = 1, 2, \ldots, t\}$. To detect an upward mean shift the CUSUM chart is applied with the following statistic

$$C_t^+ = \max(0, C_{t-1}^+ + (X_t - \mu_0) - k) \tag{2.5}$$

with $C_0^+ = 0$. The control chart gives a signal of an upward mean shift when

$$C_t^+ > h$$

where k and h are the allowance and the control limit respectively as we mentioned before. To detect a downward mean shift in the process, the form of the CUSUM chart would have the charting statistic

$$C_t^- = \min(0, C_{t-1}^- + (X_t - \mu_0) + k) \tag{2.6}$$

where $C_0^- = 0$. This chart gives a signal of a downward mean shift if

$$C_t^- < -h$$

Figure 2.2 shows a basic example for a CUSUM control chart simulating a process where we see 20 observations from $N(10, 1)$ and then we observe ten observations from $N(11, 1)$, that is a 1σ shift in the mean of the process. We see an increase in the tendency of the process; the red points indicate the presence of an Out-of-control signal in the twenty-four and twenty-five observations. Furthermore, in the nineteenth observation, we observe an upward change point in the process.

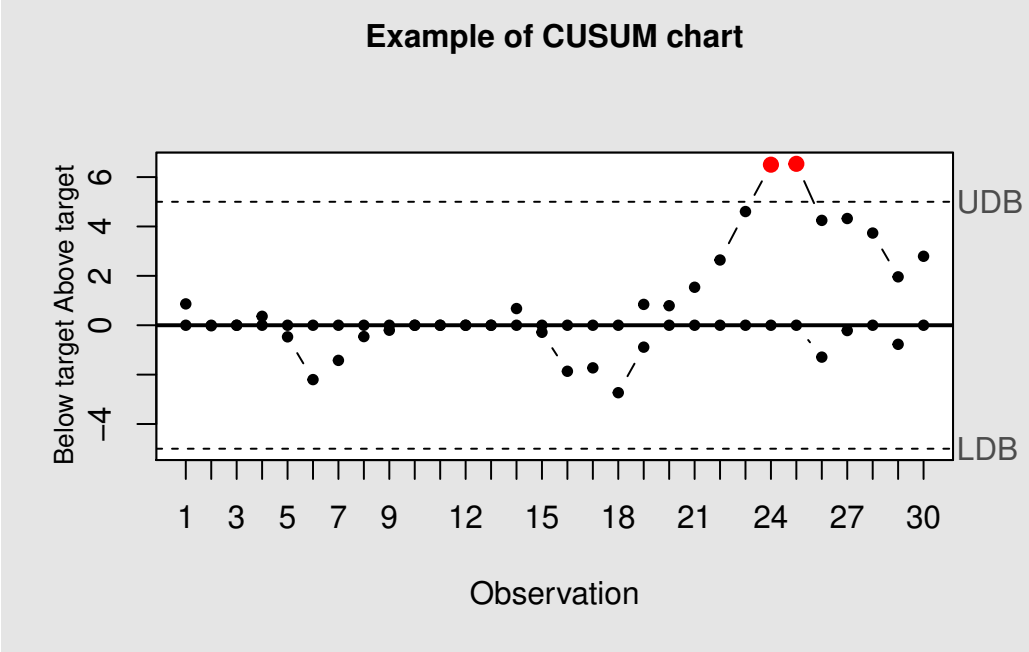

Figure 2.2: Example of a CUSUM chart

Another excellent alternative for Shewhart control charts, to detect small to moderate shifts in the process, is the exponentially weighted moving average (EWMA) control

charts. Roberts, 1959 proposed this control chart, that is constructed based on a weighted average of all observed data available at the current time point. Under normality, if the in control distribution has a mean of μ and standar deviation of σ, the charting statistic for the EWMA control chart is: for $n \geq 1$

$$E_n = \lambda X_n + (1 - \lambda) E_{n-1}$$

where $E_0 = \mu_0$ and $\lambda \in (0, 1]$ is the weighting parameter. The basic control limits for detect a mean shift are:

$$UCL = \mu_0 + L\sqrt{\frac{\lambda}{2-\lambda}(1 - (1-\lambda)^{2n})\sigma} \tag{2.7}$$

$$CL = \mu_0 \tag{2.8}$$

$$LCL = \mu_0 - L\sqrt{\frac{\lambda}{2-\lambda}(1 - (1-\lambda)^{2n})\sigma} \tag{2.9}$$

where $L > 0$ is a design parameter. Figure 2.2 shows a basic example of the look of an EWMA control chart with $\lambda = 0.1$ and a design parameter $L = 2.454$. We plot E_n for a sample of size 30 where the center dashed line is the target mean $\mu_0 = 10$. In observation eighteen, we see an upward trend in the process, indicating a possible change to the Out-of-control state because all the following statistics are above the upper control limit. For more details about these control charts see, Qiu, 2014.

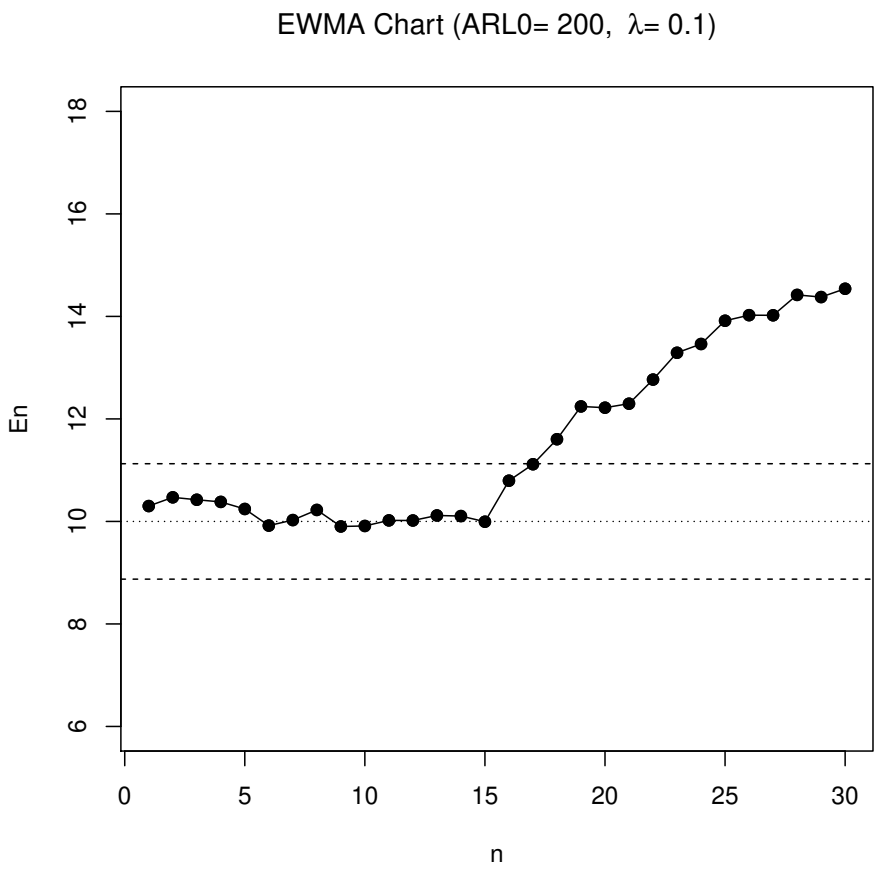

Figure 2.3: Example of an EWMA control chart

2.2 Traditional Approach and PTP variability

Statistical Process Control (SPC) methods are widely used to monitor and improve the production process and are adopted in many industries. Most SPC methods involve parameter estimation to design a control chart, such as the mean and standard deviation of the process. These parameters must be estimated from a Phase I reference sample collected when the process is presumably in control.

When parameters are estimated, the performance of the control chart is negatively affected compared with the unrealistic case of known parameters. More precisely, the most popular performance metric, the ARL_0 (the in-control average run length or, in other words, the average number of samples monitored until the control chart triggers a false alarm), is significantly affected by the parameter estimation. A review of the effects

of parameter estimation on control chart properties can be seen in Jensen et al., 2006 and Psarakis et al., 2014. Many research works have already documented the impacts of estimation errors and the urgent need to consider practitioner-to-practitioner variability (PTP); since different practitioners obtain different samples, their estimations and control limits will vary, and as a consequence, the control chart performance will be variable. For a comprehensive discussion about PTP and parameter estimation, see Capizzi and Masarotto, 2020 and Faria Sobue et al., 2020.

More recently, an alternative point of view has emerged that suggests focusing on the performance of the control chart given the data from which the parameters are estimated, and the control limits are constructed. This approach is known as the conditional performance perspective, in which the focus is on the in-control run length distribution conditioned on a given estimate of the parameters. And consequently on its various attributes such as its mean, i.e., the conditional in-control average run length (i.e., on the $CARL_0 = E(RL_0|\hat{\mu}, \hat{\sigma})$ distribution). Recently, authors argued that the conditional perspective is more meaningful in the chart design because it considers the practitioner-to-practitioner variability (PTP), which is not considered by the traditional unconditional approach. Figure 2.4 shows a simulation example to see the spread of the empirical distribution of conditional ARL for a Shewhart $\bar{X}$ control chart with estimated parameters. We simulate 1000 reference samples (1000 practitioners) of size ten and monitoring samples of size 10. As we can see, the desired in-control ARL_0 is fixed at 370, but for most of the cases, more precisely for 60% of the simulated reference samples, the control chart triggers a false alarm before the desired moment. This performance of the control chart is inadequate. Thus practitioners cannot be sure about the expected performance when implementing a control chart to their processes.

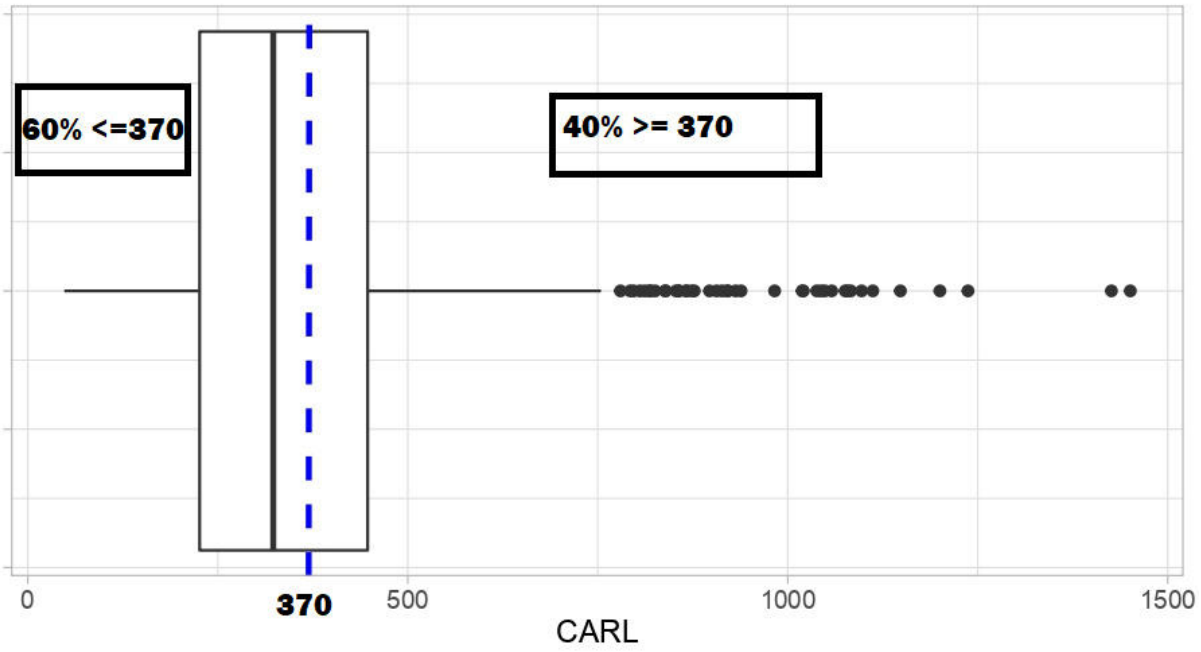

Figure 2.4: Conditional ARL simulation example

The conditional perspective argues that the conditional in-control run length distribution and consequently its attributes such as the conditional average run length $CARL_0$ are more meaningful in the context of the chart design with estimated parameters. Recognizing the fact that the $CARL_0$ is a random variable, one frequently used performance measure under the conditional perspective has been the so-called **exceedance probability criterion** (EPC), see (Albers and Kallenberg, 2005 and Albers et al., 2005). Under which the probability that the $CARL_0$ is greater than some desirable nominal value (such as 370.4) is high. Jardim et al., 2020 evaluated the conditional perspective for a Shewhart $\bar{X}$ chart with estimated parameters in which they state the EPC in the following way

$$P(CARL_0 \geq \frac{1}{\alpha}) = 1 - p$$

for a small p value (such as 0.05) and α is equal to the nominal false alarm rate. This ensures, for example, that $CARL_0$ is at least equal to a nominal value such as 370.4, with a high probability. This assures that for charts constructed under the EPC, unacceptably low $CARL_0$ values will not be very likely, so that there is no need to worry about a large number of false alarms. Celano and Chakraborti, 2020 adequate this formulation for EPC to the FHP processes context, and we use this FHP formulation of the EPC in this thesis to generate the guaranteed control limits under the conditional perspective for the proposed control chart.

2.3 Finite Horizon Production Processes

In industry, there exist processes in which the number of scheduled inspections before it ends should be restricted to a few tens. These processes are known as finite horizon production processes (FHP). There are many reasons why the SPC researchers have focus their attention on study this kind of processes; for us, the most important ones are:

- Finite production runs usually start without any knowledge or partial availability of historical data about the distribution of the quality parameter to be monitored.
- Due to the characteristics of these processes, the non-parametric control charts have been the most studied type of control charts.
- These kinds of processes are widespread in the industry, and they are present in baby diaper companies, the automotive sector, job-shop, and a small lot of production.

Statistical process monitoring of these processes presents some important issues for practitioners:

- There is no clear distinction between the Phase I and Phase II implementation of the control chart: online monitoring is immediately started on a finite number of samples I without performing any retrospective study.
- Long run measures of chart performance like the Average Run Length (ARL) are inappropriate for an FHP process.

2.3.1 Control Charts for FHP processes

Many authors have proposed control charts for monitoring finite horizon productions. Nevertheless, almost all of them have assumed the known parameter case. Under the assumption of normal observations, Shewhart-type control charts have been investigated, see, Celano et al., 2016. Also, CUSUM control schemes for short-run productions have been proposed, see Nenes and Tagaras, 2010. More recently, Shewhart-type, Student's t and F control charts have been discussed, see Celano and Castagliola, 2018b, Celano et al., 2011, Celano and Castagliola, 2018a. But, these assumptions cannot be made for these types of processes. To have a robust In-control performance when the distribution of the quality parameter is unknown, as in FHP processes, implementing distribution-free control charts may be a better solution for online monitoring.

The application of distribution-free control charts to FHP processes is still very limited in the SPM literature. Most of them focus on the online monitoring of a specified location parameter. Some examples of these control charts are the Shewhart and EWMA sign control charts that have been implemented in the FHP context by considering a deviation from a specified target value, see Celano and Chakraborti, 2020 and Celano et al., 2015. References on detail are revised in section 2.3

2.3.2 Measures of Performance for FHP processes

Over the last decade, authors have proposed many different metrics of performance for FHP. Here, we will consider the most common performance metrics: False Alarm Probability (FAP) for the In-control state and True Signal Probability by the End of the Run for the Out-of-control state. In this work, we want to obtain a guaranteed performance of the control chart, so we are going to use conditional metrics of performance, defined as follows:

During a finite production horizon run with I scheduled inspections, we are interested in fixing the probability $FAP(I)$ at a small nominal value, denoted as FAP_0. The false alarm probability is a random variable conditional on the reference sample $X = x$. We call it the conditional FAP and denoted as $CFAP(x|I)$ for $X = x$. We have

$$CFAP(x|I) = 1 - (1 - \alpha)^I \tag{2.10}$$

(where α is the false alarm rate at each inspection), that is, given the reference sample $X = x$, $CFAP(x|I)$ is equal to the probability that the Lepage-Mood control chart triggers at least one false alarm signal for a process operating in the In-Control state up to the end of the production run.

When a shift either in location or scale or both simultaneously and the process goes to an Out-of-control state, practitioners want to have a high true signal probability of detecting the process change-point as soon as possible. Practitioners are interested in the probability of a true signal by the end of the run (RSP), as was stated in Celano and Castagliola, 2018a and Celano and Castagliola, 2018b. The true signal probability by the end of the run RSP depends on β (probability of a true signal at each scheduled inspection). Thus, it is a random variable conditional on the reference sample as was stated in Celano and Chakraborti, 2020. We denote this conditional signal probability as $CRSP(x|c, I)$ and is computed as:

$$CRSP(x|c, I) = 1 - (1 - \beta)^{I-c+1} \tag{2.11}$$

(where c is the moment when the process goes to the Out-of-control state), that is the probability that the control chart triggers a true signal by the end of the run.

In this work, as it was considered in Celano and Chakraborti, 2020 we also use the unconditional values of $FAP(I)$, and $RSP(c, I)$ as metrics for the performance of the proposed control chart.

In practice, the true distributions of the conditional measures are unobservable. Therefore, they need to be estimated through a Monte Carlo simulation generating R reference samples $x^{(r)}$, with $r = 1, 2, \ldots, R$. This simulation allows us the get the empirical distributions of $CFAP(x^{(r)}|I)$ and $CRSP(x^{(r)}|c, I)$ and their quantiles to be estimated. Then, the unconditional measures of performance for the In-control analysis can be calculated as:

$$\widehat{UFAP}(I) = \frac{1}{R}\sum_{r=1}^{R} CFAP(x^{(r)}|I) \tag{2.12}$$

2.3.3 Lepage-type statistics

In this research we are interested in the detection of shifts in location and scale of a process. The Lepage test is one of the most popular distribution-free tests for joint monitoring location and scale in the two-sample problem. The Lepage test was first introduced by Lepage, 1971, and combines the standardized versions of the Wilcoxon-Rank sums statistic, as an statistic used in the two sample location test, and the Ansari-Bradley statistic, as an statistic used in the two sample scale test. Recent work by Conover et al., 2018 analyzed some other combinations for Lepage-type statistics with other nonparametric statistics used in tests for scale, including four non-parametric rank tests: the Ansari-Bradley test, the Mood test, and the Klotz test. Of these four tests, the Mood test for spread had slightly better average performance than the other three in terms of power for detecting differences in the spread. Thus, it is reasonable to use the Mood statistic paired with the Wilcoxon-Rank sums statistic instead of the Ansari-Bradley statistic in a Lepage-type statistic for detecting changes in location or scale in a conditional scheme for monitoring finite horizon production processes (FHP). In this work, we use the squared standardized versions of Wilcoxon-Rank sums statistic and Mood statistic in our proposed control chart.

2.4 Literature Review for FHP Processes

Table 2.1: Control Charts for FHP processes

Paper	Author(s)	Year	Application	Statistic	Type of Chart
Shewhart and EWMA t control charts for short production runs	Giovanni Celano, Philippe Castagliola, Enrico Trovato, Sergio Fichera	2010	Yes	T - Student's t distribution	Shewhart and EWMA
Evaluation of CUSUM Charts for Finite-Horizon Processes	George Nenes, George Tagaras	2010	Yes	C - CUSUM statistic	CUSUM
The Variable Sampling Interval control chart for finite horizon processes	George Nenes, Philippe Castagliola, Giovanni Celano, Sofia Panagiotido	2013	Yes	Sample Mean	Variable Sampling Interval Shewhart
The performance of the Shewhart sign control chart for finite horizon processes	Giovanni Celano, Philippe Castagliola, Subha Chakraborti, George Nenes	2015	Yes	Sign	Shewhart
Economic and Statistical Design of Vp Control Charts for Finite-Horizon Processes	George Nenes, Philippe Castagliola, Giovanni Celano	2016	No	Sample Mean	Shewhart
Joint Shewhart control charts for location and scale monitoring in finite horizon processes	Giovanni Celano, Philippe Castagliola, Subha Chakraborti	2016	Yes	Sign, Wilcoxon Signed-Rank, Student's t, Downton's estimator, Average absolute deviation from median MD, Sample variance	Shewhart
An EWMA sign control chart with varying control limits for finite horizon processes	Giovanni Celano, Philippe Castagliola	2018	Yes	Sign	EWMA
A distribution-free Shewhart-type Mann-Whitney control chart for monitoring finite horizon productions	Giovanni Celano, Subhabrata Chakraborti	2020	Yes	Mann-Whitney	Shewhart

Online monitoring of processes with finite horizon production is a challenging quality control issue. Thus, researchers have started to turn their attention to solving the problems in monitoring a finite horizon production process since this type of process usually runs without any knowledge or partial availability of historical data about the distribution of the quality parameter. To that, Nenes and Tagaras, 2010, analyzed and evaluated a CUSUM control chart for a finite production horizon process, designed for monitoring the process mean using a parametric approach assuming normality of the underlying process. They use the sample mean $\bar{X}$ statistic to compute the CUSUM statistic. Also, they proposed statistical measures of performance for control charts that are appropriate for short runs.

Celano et al., 2011 implemented a t chart for short-run productions, assuming normality of the process, but with the advantage that the t statistic does not require the

estimation of any distribution parameter. Nenes et al., 2014, analyzed the issues involved related to the implementation of the Variable Sampling Interval (VSI) Shewhart control chart in a process with a finite production horizon. In this work, they proposed a Markov chain approach for the *exact* computation of the statistical performance of *VSI* control chart. Celano et al., 2015 evaluated the statistical performance of a non-parametric Shewhart sign control chart for monitoring the location of a quality characteristic in a production process with a finite horizon and a small number of inspections scheduled. They showed through several types of distributions of observations and different numbers of scheduled inspections the advantages of using this control chart instead of the ordinary normal theory-based Shewhart Student's t control chart. Finally, the paper of Nenes et al., 2017 presents an economic and statistical design of a *fully adaptive* Shewhart control chart. They propose a novel way to optimize the economic performance of the monitoring operation and develop a Markov chain model to compute the statistical measures of performance of the control chart.

Celano et al., 2016 compared the performance of several control charts jointly monitoring location and scale for observations with a location-scale distribution in a finite horizon process where a limited number of inspections is scheduled. For a set of symmetric distributions, their results show that the joint control charts implementing a signed-rank SR statistic and either the Downton's D estimator or the average absolute deviation MD from median generally perform the best. However, the approach of Celano et al., 2016 is developed for the case of known location and scale parameters. It does not consider a reference sample scheme, which is the main difference with this thesis. Celano and Castagliola, 2018a, implemented an EWMA control chart based on the sign statistic for monitoring the location of a quality parameter in a finite production horizon process. They computed the statistical measures of performance using a non-homogeneous Markov chain model. They presented an example that shows the advantages of implementing the proposed control chart to monitor a critical quality parameter in a bottling process. Recently, Celano and Chakraborti, 2020 implemented a Shewhart type Mann-Whitney control chart for finite production horizon processes through the Mann- Whitney statistic and a reference sample scheme. In this work, they compared the conditional performance of the control chart versus a general control chart with unconditional performance.

In recent years, the Lepage statistic has increasingly been applied in univariate non-parametric control charts, see, for example, Tercero-Gómez et al., 2020, and Mukherjee and Chakraborti, 2012. Tercero-Gómez et al., 2020 showed that the control chart based on a Lepage-type statistic using the Mood statistic outperformed the control chart based

on a Lepage-type statistic but using the Ansari-Bradley statistic instead (Chowdhury et al., 2015). Table 2.1 resumes the literature review on FHP processes considering the type of statistic, the measures of performance, and the type of control chart. We want to contribute to the literature applying the Tercero-Gómez et al., 2020 methodology with a reference sample scheme as suggested by Celano and Chakraborti, 2020 in an FHP process for joint monitoring of location and scale.

Chapter 3

Methodology

In this chapter, we describe our proposed control chart for monitoring changes in location and scale in FPH processes. The statistics used for this control chart and the one used to compare its performance are presented in Sections 3.1 and 3.2. In Section 3.3 we describe the implementation of this control chart; whereas Section 3.4 describes the process to obtain the control limits satisfying conditional and unconditional schemes. Finally, Section 3.5 presents the design of the experimentation used to evaluate the out-of-control performance.

3.1 Lepage-Mood statistic

Tercero-Gómez et al., 2020, implement a Lepage CUSUM control chart for monitoring the location and scale changes when no assumption of the distribution is known. The Lepage-Mood is constructed as follows: Let X_j, $j = 1, \ldots, m$ be a sample of independent identically distributed in-control observations obtained from a reference sample and Y_i $i = 1, \ldots, n$ be a sample of independent identically distributed observations to be evaluated as a monitored sample. The Lepage-Mood statistic, L_M is created from the sum of the *Mood* and the Wilcoxon-Rank Sums statistics described as follows:

$$Mood \quad statistic: \quad M = \sum_{j=1}^{m} \left(r(X_j) - \frac{N+1}{2} \right)^2 \tag{3.1}$$

(where $r(X)$ is the rank of the X observation in the combined sample, m is the reference sample size, n is the test sample size, and $N = m + n$.) and the Wilcoxon-Rank Sums statistic (Tercero-Gómez et al., 2020):

$$WRS_{st} = \frac{T_1 - \mu_1}{\sigma_1} \tag{3.2}$$

where

$$T_1 = \sum_{i=1}^{m} r(X_{1i}) \tag{3.3}$$

$$\mu_1 = m \cdot \frac{N+1}{2} \tag{3.4}$$

$$\sigma_1 = \sqrt{\frac{m \cdot n \cdot (N+1)}{12}} \tag{3.5}$$

Figure 3.1 shows an example to see that the WRS increases when we have a mean shift. We simulate ten test samples of size ten from a $N(0,1)$ distribution and ten test samples of size ten from a $N(1,1)$ distribution and compute the WRS for these test samples with a reference sample of size 30 from the $N(0,1)$ distribution. As we can see, the WRS statistic is a reasonable choice to detect location shifts in the process.

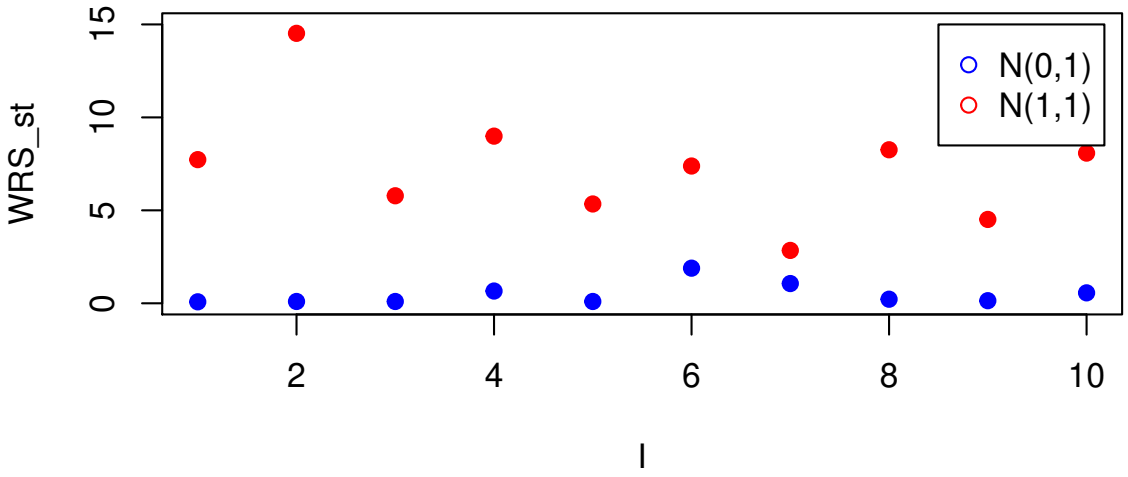

Figure 3.1: WRS statistic

We obtain the standardized version of the $Mood$ statistic by subtracting its mean and dividing by its standard deviation to obtain

$$M_{st} = \frac{M - \mu_M}{\sigma_M} \tag{3.6}$$

where

$$\mu_M = m \cdot \frac{N^2 - 1}{12} \tag{3.7}$$

and

$$\sigma_M^2 = \frac{m \cdot n \cdot (N+1) \cdot (N^2 - 4)}{180}. \tag{3.8}$$

Figure 3.2 illustrates how the *Mood* increases when we have a scale shift. We simulate ten test samples of size ten from a $N(0,1)$ distribution and ten test samples of size ten from a $N(0,1)$ distribution and compute the *Mood* for these test samples with a reference sample of size 30 from the $N(0,2)$ distribution. As we can see, the *Mood* statistic is a reasonable choice to detect scale shifts in the process.

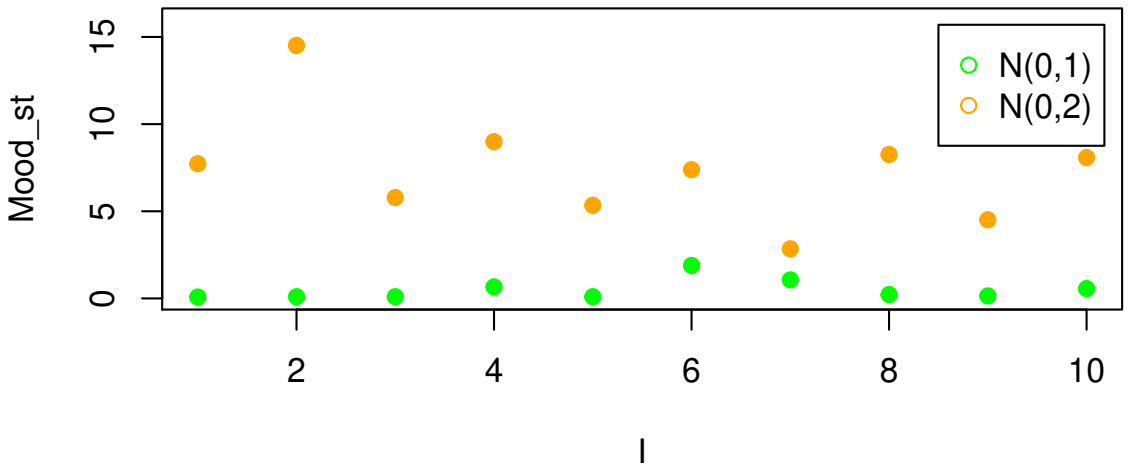

Figure 3.2: Mood statistic

These two statistics are combined to calculate the Lepage-Mood statistic as

$$L_M = WRS_{st}^2 + M_{st}^2. \tag{3.9}$$

Tercero-Gómez et al., 2020 show that with this statistic, the control chart has an outstanding performance in terms of the power of detection changes in both the location and scale parameters. Figure 3.3 shows how the Lepage-Mood statistic change when we have both location and scale shifts making the combination of WRS and *Mood* statistic an excellent alternative to detect both location and scale shifts in the process.

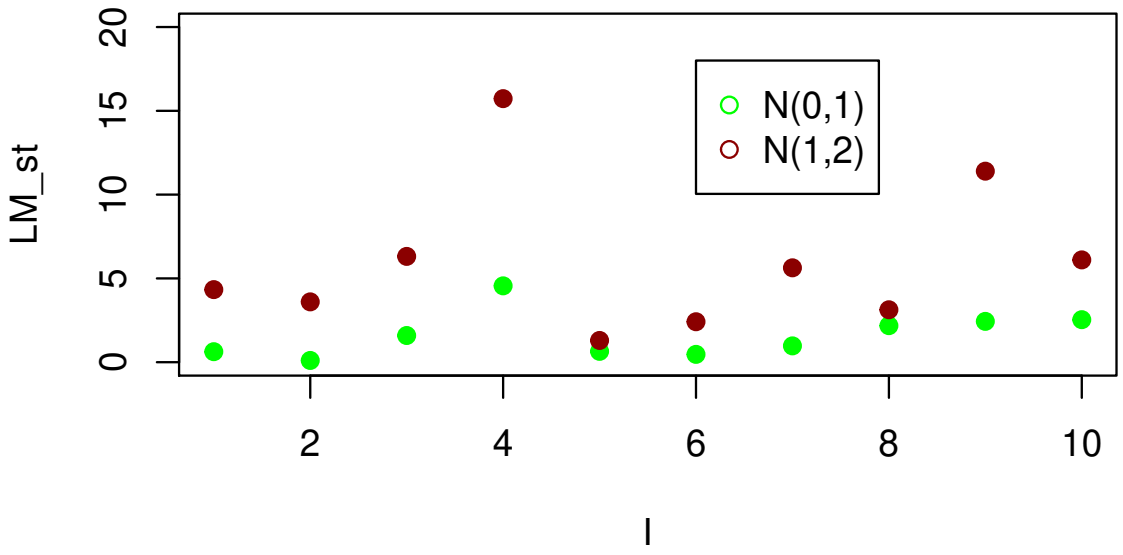

Figure 3.3: Lepage-Mood statistic

When there are ties in the data, Hollander et al., 2013 explains that there is no change in the equations for the expected value of the statistics, but for the variance, the equations are a little different, and need to be modified by the ones in, page 118 Hollander et al., 2013.

3.2 Lepage-Ansari-Bradley statistic

This subsection describes the Lepage statistic that we use to compare our proposed control chart in the Out-of-control performance study. In the same manner, as in the above subsection, the Lepage-Ansari-Bradley statistic, L_{AB} is created from the sum of the standardized versions of the WRS(explained in 3.1) and the AB statistics as

$$L_{AB} = WRS_{st}^2 + AB_{st}^2 \tag{3.10}$$

where

$$AB_{st} = \frac{T_2 - \mu_2}{\sigma_2}, \tag{3.11}$$

with

$$T_2 = \sum_{j=1}^{m} |r(X_j) - \frac{N+1}{2}|, \tag{3.12}$$

$$\mu_2 = \begin{cases} \frac{m(N+2)}{4}, & if \quad N \quad is \quad even \\ \frac{m(N+1)^2}{4N}, & if \quad N \quad is \quad odd \end{cases} \tag{3.13}$$

$$\sigma_2 = \begin{cases} \frac{mn(N^2-4)}{48(N-1)}, & if \quad N \quad is \quad even \\ \frac{mn(N+1)(N^2+3)}{48N^2}, & if \quad N \quad is \quad odd \end{cases} \tag{3.14}$$

Figure 3.4 illustrates, as in the *Mood* statistic example, how the Ansari-Bradley statistic increases when we have a scale shift in the process, so the Ansari-Bradley statistic is another alternative to detect scale shifts in the process.

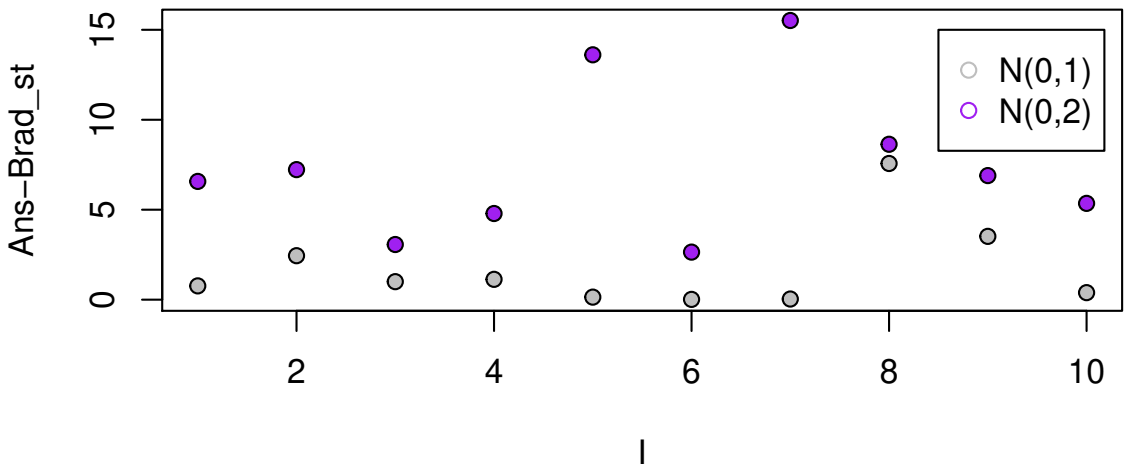

Figure 3.4: Ansari-Bradley statistic

Figure 3.5 shows an example of how the Lepage-Ansari-Bradley statistic increases when we have both a location and scale shifts in the process. Thus, it is natural to compare the performance of the control chart based on the Lepage-Mood statistic with the Lepage-Ansari-Bradley statistic.

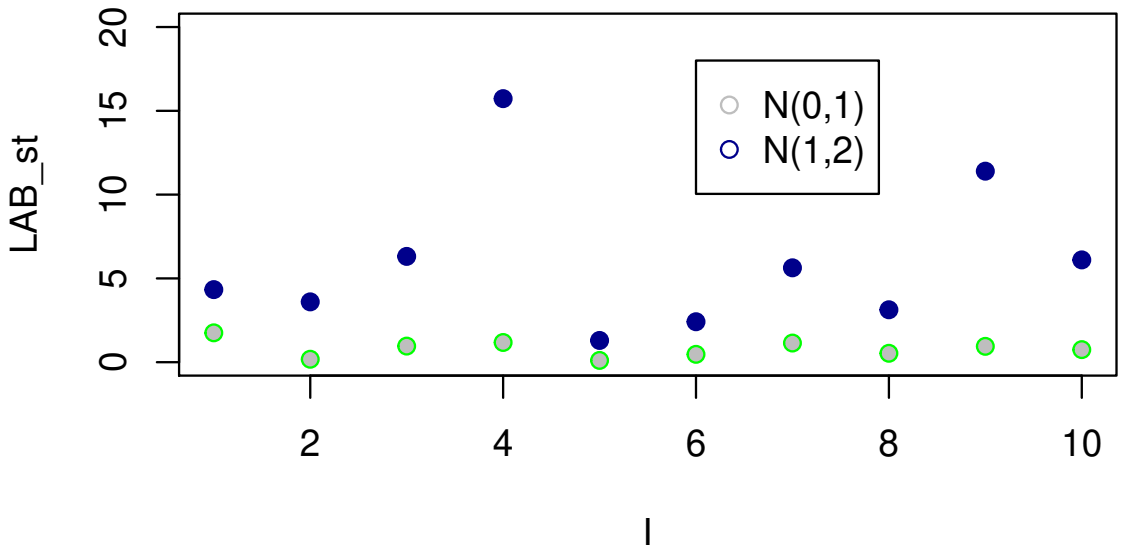

Figure 3.5: Lepage-Ansari-Bradley statistic

3.3 Implementation of the Shewhart Lepage control chart in an FHP process

We consider that a lot of L parts should be produced by H hours. A finite number of inspections are scheduled during the production run. Statistical process monitoring is performed using a Shewhart Lepage-Mood control chart on a continuous quality characteristic to check if its location and scale are in control during the production run. Online monitoring is started by collecting a reference sample $X = (X_1, X_2, \ldots, X_m)$ of m i.i.d observations from some unknown continuous cumulative distribution function F. At each scheduled inspection i, a test sample $Y_i = (Y_{i,1}, Y_{i,2}, \ldots, Y_{i,n})$, for $i = 1, \ldots, I$ is collected every $h = \frac{H}{I}$ hours from an unknown continuous distribution G_i.

Then, at each scheduled inspection, compute the corresponding Lepage-Mood statistic:

$$L_M^i(X, Y) = WRS_{st}^2(X, Y) + M_{st}^2(X, Y) \tag{3.15}$$

A signal is presented when $L_M^i \geq L_{m,n}$, where the control limit $L_{m,n}$ is defined to obtain a desired performance, as is seen in next subsection. Also, we can compute the L_{AB}^i statistic in the same manner as L_M^i statistic only changing M_{st} statistic for AB_{st} statistic.

To measure the performance of our proposed control chart, we need to compute the α and β probabilities to obtain the conditional False Alarm (CFAP) Probability and the conditional True Signal Probability by the end of the Run (CRSP).
Given the reference sample $X = x$ collected to run the proposed Lepage-Mood control chart, the false alarm rate at each inspection i, for $i = 1, \ldots, I$ is:

$$\alpha = \frac{N_\delta}{N \cdot I}$$

where $N_\delta = \sum_{k=1}^{N} \sum_{i=1}^{I} \ell(L_M^i > L_{m,n})$ (where $\ell(\cdot)$ is an indicator function) is the number of signals in the Monte Carlo simulation study, N is the total replicates of the simulation and I is the number of scheduled inspections. A signal is triggered when $L_M^i > L_{m,n}$ for a given reference sample $X = x$ and I test samples x_n. This false alarm rate (FAR) is a random variable conditional on the reference sample $X = x$, as it was stated in Celano and Chakraborti, 2020. Then, we compute the CFAP as in 2.10.

For the Out-of-control analysis, we need to compute the probability β, then, given the reference sample $X = x$ collected to run the proposed Lepage-type control chart, the probability β of a true signal at each scheduled inspection is given by

$$\beta = \mathcal{P}_G(L_M^i > L_{m,n}) \tag{3.16}$$

where $\mathcal{P}_G(L_M^i > L_{m,n})$ is estimated using Monte Carlo simulation using the control limits obtained in the in-control analysis. To get the Out-of-control performance, we perform a simulation over shift sizes in both location and scale, δ, τ respectively, and when the process change-point c occurs before the scheduled end of the production run. Then, we compute the CRSP as in 2.11.

3.4 In-control performance

The choice of the control limit $L_{m,n}$ is related to the empirical distribution of $CFAP(x|I)$. Under the conditional perspective, the control limit is selected following an exceedance probability criterion, see Jardim et al., 2020, guaranteeing that

$$Pr(CFAP(x^{(r)}|I) \geq FAP_0) = 1 - \frac{q}{100} \tag{3.17}$$

that is, $\widehat{CFAP}_q(I) = FAP_0$, where $\widehat{CFAP}_q(I)$ is the *qth* quantile of the empirical distribution of $CFAP(x^{(r)}|I)$. Here, we assume $\frac{q}{100} = 0.95$, that is $\widehat{CFAP}_{95}(I) = FAP_0$. This means that, given the reference sample $X = x$, the selected control limit guarantee that $FAP(I) \leq FAP_0$ with a probability $p = 0.95$.

Under the unconditional scheme, the control limit $L_{m,n}$ is selected to meet the following constraint:

$$\widehat{UFAP}(I) = \frac{1}{R}\sum_{r=1}^{R} CFAP(x^{(r)}|I) = FAP_0 \tag{3.18}$$

The method for finding the control limit $L_{m,n}$ is based on the classical bisection method stopping the search when (3.17) and (3.18) are met for the conditional and unconditional schemes respectively.

Once the control limit $L_{m,n}$ is selected, we estimate the standard deviation $\widehat{SDFAP}(I)$, the *50th*, *75th* and *95th* quantiles, denoted by $CFAP_{50}(I)$, $CFAP_{75}(I)$ and $CFAP_{95}(I)$ from the empirical distribution of $CFAP(x^{(r)}|I)$.

$$SDFAP = \sqrt{\frac{\sum_{r=1}^{R}\left[CFAP(x^{(r)}|I) - UFAP(I)\right]^2}{R-1}} \tag{3.19}$$

where R is the number of simulated reference samples and

$$UFAP(I) = \frac{1}{R}\sum_{r=1}^{R} CFAP(x^{(r)}|I). \tag{3.20}$$

3.5 Out-of-control analysis

We evaluate the Out-of-control performance of the proposed Shewhart Lepage-type control chart in three cases: (i) when only mean changes, (ii) when only standard deviation changes, and (iii) when both mean and standard deviation changes. For the $R = 1000$ simulated reference samples, we obtain the empirical distribution of $CRSP(x^{(r)}|c, I)$, $r = 1, \ldots, R$ with different shift sizes δ and τ for the process location and scale respectively. After this, we use the distribution of $CRSP(x^{(r)}|c, I)$ to get measures about the conditional Out-of-control performance based on its quantiles. As in Celano and Chakraborti, 2020 we consider two process change point scenarios: when an assignable

cause occurs before the first scheduled inspection ($c = 1$) and when the assignable cause occurs after one half the production ($c = \frac{I}{2} + 1$). For a lot size of $L = 1000$, we plotted the trend of the **median** $RSP_{50}(c, I)$ vs δ and τ. The measure $RSP_{50}(c, I)$ is considered to evaluate the Out-of-control performance of the Shewhart Lepage-type control chart for 50% of the simulated reference samples. We use a $FAP_0 = 0.1$ and $I = 10$ scheduled inspections. With this settings, the parts available for two consecutive inspection are $L_h = 100$ and we consider a reference sample size of $m = 30$ and $m = 70$ to create our plots. The control limits with the L_{AB} statistic were calibrated with the conditional scheme and only for the proposed Out-of-control scenarios, so the results are comparable.

In the next section, the performance analysis of the proposed control chart is presented. For the In-control analysis, we present tables with the control limits for the conditional and unconditional schemes using the Lepage-Mood statistic. For the Out-of-control analysis, we present a performance comparison between our proposed control chart with the Lepage-Mood statistic and the alternative of using the Lepage-Ansari-Bradley statistic.

Chapter 4

Results and Discussion

In this chapter, we perform a Monte Carlo simulation study to evaluate the performance of the proposed control chart. We described the considered scenarios for both the IC and OOC analysis in section 4.1. In subsection 4.2.1, we present the IC results for various scenarios with different reference sample sizes and test sample sizes. Finally, in subsection 4.2.2, we expose several plots to illustrate the OOC performance of the control chart under different sample sizes and distributions.

4.1 Simulation Design

In this section, we evaluate the statistical performance of the proposed Shewhart Lepage-type control chart for different FHP scenarios. We consider several scenarios formed by the next parameters for the In-control analysis:

- lot size of $L = \{1000, 10000\}$ parts to be produced
- Target false alarm probability $FAP_0 = 0.1$
- Number of scheduled inspections $I = \{10, 20, 50\}$
- Reference sample size $m = \{20, 30, 40, 50, \ldots, \min(0.9 \times \frac{L}{I}, 500)\}$
- Test sample size $n = \{5, 10, 25\}$
- Number of simulated reference samples $R = 1000$

In the Out-of-control analysis, we also consider observations from the following four distributions:

- *Symmetric.* Standard Normal, $N(0, 1)$ and Student's t, $t(4)$
- *Asymmetric.* $Gamma(2, 1)$ and $Gamma(3, 1)$

4.2 Results

4.2.1 In-Control Results

In this section, we compare the conditional statistical performance of our proposed control chart with the common unconditional scheme to see the advantages of considering the "exceedance probability criterion" in the practitioner-to-practitioner variability.

Table 4.1: Control limits under the conditional perspective for the proposed Lepage-type control chart with $FAP_0 = 0.1$, lot size = 1000 parts, $CFAP_{95} = 0.1$

I	m	n	$L_{m,n}$	$SDFAP$	$CFAP_{50}$	$CFAP_{75}$
10	20	5	11.4625	0.0431	0.0056	0.0196
		10	10.75	0.0567	0.0032	0.0140
	30	5	11.75	0.0404	0.0105	0.0286
		10	11.25	0.0519	0.0052	0.0202
	40	5	11.9	0.0392	0.0141	0.0307
		10	11.8125	0.0459	0.0064	0.0186
	50	5	11.925	0.0324	0.0174	0.0380
		10	11.7	0.0381	0.0102	0.0279
	60	5	11.5005	0.0340	0.0249	0.0474
		10	11.3	0.0410	0.0163	0.0374
	70	5	11.75	0.0345	0.0254	0.0473
		10	11.6875	0.0423	0.0158	0.0364
	80	5	11.6	0.0294	0.0294	0.0486
		10	11.6	0.0333	0.0194	0.0383
	90	5	11.45	0.0299	0.0317	0.0506
		10	11.45	0.0346	0.0207	0.0399
20	20	5	12.7310	0.0499	0.0041	0.0201
		10	12.05	0.0566	0.0017	0.0082
	30	5	13.25	0.0485	0.0092	0.0268
		10	12.625	0.0608	0.0040	0.0165
	40	5	13.25	0.0402	0.0143	0.0327
		10	12.75	0.0522	0.0071	0.0227

Table 4.2: Control limits under the unconditional perspective for the proposed Lepage-type control chart with $FAP_0 = 0.1$, lot size = 1000 parts, $UFAP = 0.1$

I	m	n	$L_{m,n}$	$SDFAP$	$CFAP_{75}$	$CFAP_{95}$
10	20	5	8	0.1266	0.1443	0.3931
		10	7.95	0.1280	0.1097	0.3804
	30	5	8.625	0.1075	0.1254	0.3131
		10	8.25	0.1276	0.1128	0.3407
	40	5	8.75	0.0962	0.1420	0.3016
		10	8.5	0.1130	0.1272	0.3338
	50	5	8.9	0.0843	0.1298	0.2697
		10	8.45	0.1057	0.1299	0.3189
	60	5	9.05	0.0769	0.1316	0.2580
		10	8.85	0.0947	0.1184	0.2958
	70	5	9.2	0.0657	0.1246	0.2195
		10	8.7	0.0864	0.1290	0.2677
	80	5	9.05	0.0657	0.1289	0.2284
		10	8.8	0.0812	0.1225	0.2541
	90	5	9.15	0.0599	0.1282	0.2128
		10	8.9	0.0749	0.1263	0.2497
20	20	5	9.5	0.1397	0.1167	0.3819
		10	8.925	0.1567	0.0994	0.4242
	30	5	10.15	0.1187	0.1349	0.3215
		10	9.625	0.1389	0.1153	0.3562
	40	5	10.35	0.1048	0.1259	0.3067
		10	9.6	0.1367	0.1280	0.3989

Table 4.3: Control limits under the conditional perspective for the proposed Lepage-type control chart with $FAP_0 = 0.1$, lot size = 10000 parts, $CFAP_{95} = 0.1$

I	m	n	$L_{m,n}$	$SDFAP$	$CFAP_{50}$	$CFAP_{75}$
20	30	5	13.25	0.0416	0.0084	0.0252
		10	12.75	0.0516	0.0031	0.0143
		25	12.3	0.0645	0.0027	0.0112
	50	5	13.52	0.0351	0.0157	0.0338
		10	13.21	0.0401	0.0078	0.0248
		25	12.52	0.0517	0.0055	0.0186
	100	5	13.28	0.0313	0.0306	0.0521
		10	13.22	0.0355	0.0198	0.0423
		25	13.04	0.0425	0.0101	0.0271
	150	5	12.81	0.0270	0.0427	0.0621
		10	12.75	0.0307	0.0316	0.0534
		25	12.59	0.0376	0.0185	0.0399
	200	5	12.67	0.0257	0.0467	0.0651
		10	12.595	0.0297	0.0361	0.0569
		25	12.64	0.0345	0.0222	0.0422
	350	5	12.314	0.0226	0.0575	0.0731
		10	12.24	0.0266	0.0473	0.0659
		25	12.216	0.0331	0.0341	0.0545

Table 4.4: Control Limits under the unconditional perspective for the proposed Lepage-type control chart with $FAP_0 = 0.1$, lot size = 10000 parts, $UFAP = 0.1$

I	m	n	$L_{m,n}$	$SDFAP$	$CFAP_{75}$	$CFAP_{95}$
10	30	5	8.63	0.1075	0.1254	0.3131
		10	8.25	0.1276	0.1128	0.3407
		25	8.45	0.1580	0.0979	0.4318
	50	5	8.9	0.0843	0.1298	0.2697
		10	8.45	0.1057	0.1299	0.3189
		25	8.76	0.1371	0.1262	0.3992
	100	5	9.34	0.0547	0.1214	0.2074
		10	8.96	0.0698	0.1267	0.2451
		25	8.8	0.0880	0.1211	0.2870
	150	5	9.325	0.0460	0.1200	0.1794
		10	8.85	0.0625	0.1309	0.2235
		25	8.885	0.0778	0.1161	0.2525
	200	5	9.27	0.0408	0.1211	0.1778
		10	9.11	0.0511	0.1179	0.1949
		25	9.005	0.0658	0.1145	0.2351
	350	5	9.325	0.0295	0.1132	0.1535
		10	8.95	0.0392	0.1250	0.1795
		25	9.03	0.0456	0.1170	0.1935
	500	5	9.16	0.0262	0.1211	0.1513
		10	9.06	0.0315	0.1153	0.1539
		25	8.95	0.0375	0.1178	0.1731

Table 4.5: Control limits under the conditional perspective for the proposed Lepage-type control chart with $FAP_0 = 0.1$, lot size = 10000 parts, $CFAP_{95} = 0.1$

I	m	n	$L_{m,n}$	$SDFAP$	$CFAP_{50}$	$CFAP_{75}$
10	30	5	11.75	0.0404	0.0105	0.0286
		10	11.25	0.0519	0.0052	0.0202
		25	11.25	0.0553	0.0035	0.0144
	50	5	11.925	0.0324	0.0174	0.0380
		10	11.7	0.0381	0.0102	0.0279
		25	11.5	0.0554	0.0057	0.0183
	100	5	11.4	0.0284	0.0336	0.0528
		10	11.45	0.0325	0.0229	0.0436
		25	11.35	0.0387	0.0135	0.0308
	150	5	11	0.0260	0.0437	0.0643
		10	10.95	0.0291	0.0330	0.0538
		25	11	0.0336	0.0226	0.0426
	200	5	10.9	0.0248	0.0453	0.0634
		10	10.88	0.0290	0.0356	0.0552
		25	10.8	0.0366	0.0254	0.0468
	350	5	10.5	0.0213	0.0612	0.0759
		10	10.4	0.0252	0.0510	0.0664
		25	10.75	0.0282	0.0362	0.0538
	500	5	10.5	0.0177	0.0619	0.0742
		10	10.3	0.0205	0.0522	0.0664
		25	10.25	0.0241	0.0436	0.0607

Table 4.6: Control Limits under the unconditional perspective for the proposed Lepage-type control chart with $FAP_0 = 0.1$, lot size = 10000 parts, $UFAP = 0.1$

I	m	n	$L_{m,n}$	$SDFAP$	$CFAP_{75}$	$CFAP_{95}$
20	30	5	10.18	0.1215	0.1266	0.3833
		10	9.67	0.1458	0.1068	0.4260
		25	9.765	0.1686	0.0908	0.4896
	50	5	10.55	0.1017	0.1348	0.3190
		10	10.075	0.1291	0.1282	0.3732
		25	9.888	0.1522	0.1074	0.4338
	100	5	10.75	0.0661	0.1343	0.2331
		10	10.35	0.0852	0.1313	0.2700
		25	10.18	0.1054	0.1099	0.3161
	150	5	10.8	0.0535	0.1331	0.2097
		10	10.43	0.0691	0.1312	0.2407
		25	10.25	0.0873	0.1158	0.2728
	200	5	10.95	0.0428	0.1213	0.1790
		10	10.34	0.0590	0.1340	0.2171
		25	10.13	0.0742	0.1248	0.2694
	350	5	11.07	0.0333	0.1184	0.1627
		10	10.64	0.0440	0.1255	0.1879
		25	10.42	0.0562	0.1209	0.2173

Table 4.7: Control limits under the conditional perspective for the proposed Lepage-type control chart with $FAP_0 = 0.1$, lot size = 10000 parts, $CFAP_{95} = 0.1$

I	m	n	$L_{m,n}$	$SDFAP$	$CFAP_{50}$	$CFAP_{75}$
50	30	5	15.06	0.0436	0.0058	0.0205
		10	14.125	0.0575	0.0025	0.0139
		25	13.44	0.0662	0.0021	0.0122
	50	5	15.75	0.0398	0.0130	0.0310
		10	15.25	0.0514	0.0067	0.0216
		25	14.45	0.0666	0.0032	0.0111
	100	5	15.491	0.0336	0.0269	0.0470
		10	15.37	0.0380	0.0169	0.0359
		25	14.74	0.0519	0.0084	0.0214
	150	5	15.45	0.0302	0.0333	0.0537
		10	15.35	0.0360	0.0246	0.0447
		25	15.2	0.0470	0.0114	0.0280

Table 4.8: Control Limits under the unconditional perspective for the proposed Lepage-type control chart with $FAP_0 = 0.1$, lot size = 10000 parts, $UFAP = 0.1$

I	m	n	$L_{m,n}$	$SDFAP$	$CFAP_{75}$	$CFAP_{95}$
50	30	5	12	0.1385	0.1270	0.4247
		10	11.25	0.1645	0.0989	0.4741
		25	11.15	0.1805	0.0841	0.5323
	50	5	12.75	0.1120	0.1273	0.3445
		10	12	0.1444	0.1214	0.4116
		25	11.4	0.1691	0.1007	0.4705
	100	5	13	0.0735	0.1333	0.2469
		10	12.4	0.0973	0.1337	0.3027
		25	11.9	0.1223	0.1070	0.3469
	150	5	13.2	0.0578	0.1259	0.2126
		10	12.55	0.0788	0.1336	0.2579
		25	12.1	0.1033	0.1160	0.3011

Tables 4.2, 4.4, 4.6 and 4.8 containing the control limits $L_{m,n}$ under the unconditional perspective, also they show the standard deviation, the 75th and 95th quantiles of the empirical distribution of the $CFAP(x^{(r)}|c, I)$ denoted by $SDFAP$,$CFAP_{75}$,$CFAP_{95}$ respectively. Tables 4.1, 4.3, 4.5 and 4.7 present the same information under the conditional scheme.

In table 4.2 we can see that for $I = 10$ inspections, the 95th quantile is around 0.21 and 0.39, i.e., for the 95% of the practitioners we have an unconditional false alarm between 0.21 and 0.39, even that the average false alarm is 0.1. When $I = 20$, we this quantile is always bigger than 0.32, which is a worse performance for the 95% of the practitioners. Similar results in the 95th quantile are found in tables 4.4, 4.6 and 4.8. For table 4.4 we see that when $m \geq 200$ the value of the 75th quantile is near to 0.1, that means that the control chart under the unconditional scheme leads to a $FAP > 0.1$ for the 25% of the simulated reference samples. In tables 4.6 and 4.8 where we have $I = 20$ and $I = 50$ inspections respectively, the values in the 75th quantile are similar. In addition, in table 4.4 we see that the $SDFAP$ values increase when the test sample size n increases, and the variability among the scenarios decreases when the reference sample size increases. Also, when the number of scheduled inspections increases, the values of $SDFAP$ increase too. The behavior of $SDFAP$ is the same for tables 4.2, 4.6 and 4.8. Finally, in table 4.4 the values of the 95th quantile increases when n increases and decreases when m increases, the same happens in tables 4.2, 4.6 and 4.8. This result was first stated in Celano and Chakraborti, 2020.

Table 4.1 presents the control limits for the control chart under the conditional scheme with $I = 10$ and $I = 20$ scheduled inspections. As we expected, the control limits are wider than the ones under the unconditional scheme. We can see from tables 4.3 and 4.7 that when we increase the number of scheduled inspections, say, for instance, from ten to twenty, the control limits become wider, and the same happens from twenty to fifty inspections. These control limits guarantee that the $Pr(CFAP(x^{(r)}|c, I) \geq 0.1) = 0.05$, i.e., for the 95% of the practitioners we have a $FAP < 0.1$, so with this scheme we ensure a desired performance for practitioners. Now, in table 4.1 the $SDFAP$ values also increase when n increases and decrease when m increases. As we expected, this variability is much smaller than that presented in the unconditional scheme. For tables 4.3, 4.5 and 4.7 the $SDFAP$ values behave in the same manner.

Figure 4.1 shows the effect of the reference sample and test sample size on the probability $Pr(CFAP(x^{(r)}|I) > FAP_0)$ with the unconditional control limits. We get, $0.25 \leq Pr(CFAP(x^{(r)}|I) > FAP_0) \leq 0.40$. As reference sample size m increases, this probability tends to higher values, conversely, when the test sample size n increases. In all cases, this probability is at an unacceptable level. This contrast with the conditional scheme where the same probability $Pr(CFAP(x^{(r)}|I) > FAP_0)$ is equal, in this case, to 0.05. We can do this thanks to the "exceedance probability criterion" that allows us to fix the value of this probability as small as we want. Finally, we see that using the conditional scheme leads us to a guaranteed In-control performance of the control chart, having a low and controlled false alarm probability among all case scenarios. Contrary to the unconditional scheme, we have an increased number of false alarms because this scheme averages over the estimated parameters' distribution and does not represent the control chart's actual performance for any specific reference sample. For this reason, consider the distributions of the conditional measures of performance and their quantiles may be preferred by practitioners, see Jardim et al., 2020.

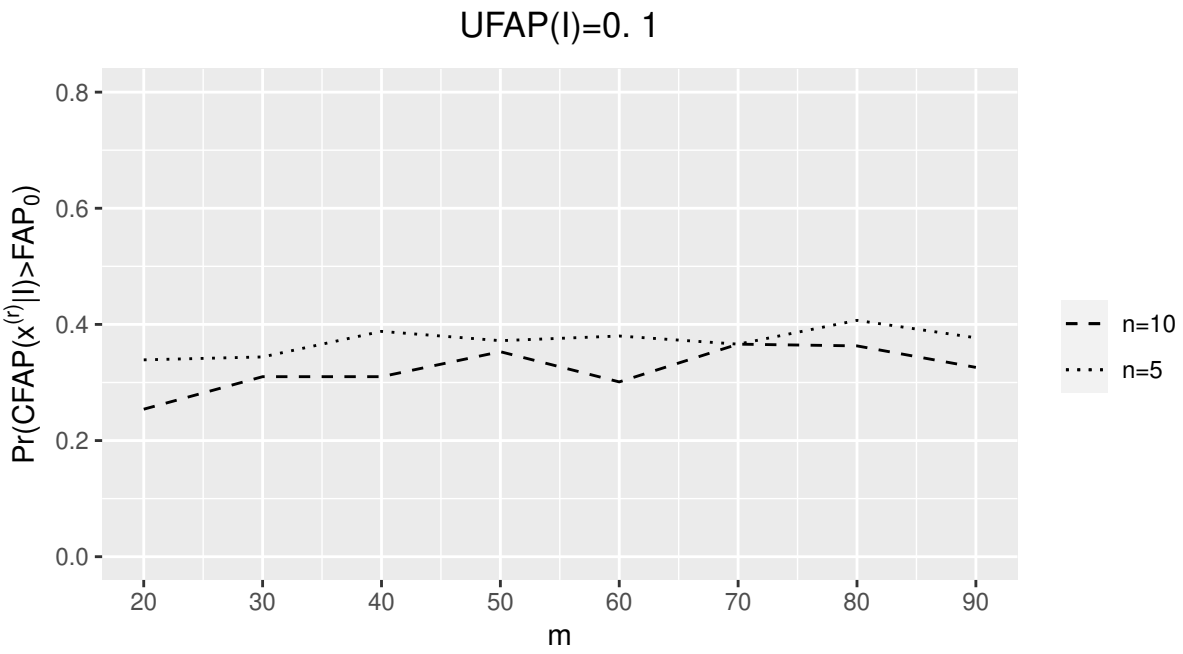

Figure 4.1: $Pr(CFAP(x^{(r)}|I) > FAP_0)$ vs m, for $L = 1000$, with the control limits selection based on unconditional FAP

4.2.2 Out-of-control Results

There is not an existent nonparametric control chart for changes in location and scale in FPH processes under the conditional perspective, hence, we use the Lepage-Ansari-Bradley statistic as this competitor to compare and measure the detection ability of true signals for the proposed control chart.

For the Out-of-control performance, we perform Monte Carlo simulations for several scenarios created with the combination of the next parameters:

- False Alarm Probability $FAP_0 = 0.1$.
- Number of scheduled inspections $I = 10$.
- Reference sample size $m = \{30, 70\}$.
- Test sample size $n = \{10, 25\}$.
- Number of simulated reference samples $R = 1000$.
- Location shift $\delta = \{0, 0.25, 0.5, 0.75, 1, 1.5, 2\}$ measured in standard deviations.
- Scale shift $\tau = \{0.25, 0.5, 1.5^{-1}, 1, 1.5, 2, 3\}$ measured as the ratio of deviationsvalidar

As we mentioned in section 3.4.1, we consider independent observations with the following distributions: standard normal, Student's with four degrees of freedom, Gamma(2,1) and Gamma(3,1) distributions.

When Only Mean Changes

Figure 4.2 shows on the y-axis the median of the empirical distribution of $CRSP(x^{(r)}|c, I)$ denoted by $RSP_{50}(c, I)$ and in the x-axis the location shift size δ for the $N(0, 1)$ distribution. In the four cases, we see that the Lepage-Mood(LM) statistic outperformed the alternative of using the Lepage-Ansari-Bradley(LAB) statistic in all scenarios. We can observe this by noting that the $RSP_{50}(c, I)$ values are higher for all considered shift sizes when considering the control chart based on the LM statistic. Now, for $m = 70$, and the change point condition (i), i.e., when a location shift occurs before the first scheduled inspection, we have a $RSP_{50}(c, I) \geq 0.99$ when $\delta \geq 1.0$ for standard normal observations using the LM statistic. For the second condition, i.e., when the shift occurs after the $\frac{I}{2}$ scheduled inspection, the control chart's performance still at a good level, for instance,

$RSP_{50}(c, I) \geq 0.82$ for $\delta \geq 1.0$. Figure 4.3 presents observations having a $t(4)$ distribution, the statistical performance is very similar, for instance, $RSP_{50}(c, I) \geq 0.99$ for $\delta \geq 1.0$ with $c = 1$ and $m = 70$. For the LAB statistic, this happens only in changes of size greater than 1.5, so it is clear that the LM statistic shows a better performance than the LAB statistic. Figures 4.4 and 4.5 presents the OOC performance of the proposed control chart for observations having asymmetrical distributions $Gamma(2, 1)$ and $Gamma(3, 1)$, respectively. In these scenarios, for both the LM statistic and LAB statistic, the control chart is less sensitive; only when we consider a test sample size, of $n = 25$ we have a robust OOC performance, for example, $RSP_{50}(c, I) \geq 0.99$ for $\delta \geq 0.75$ with the $Gamma(2, 1)$ distribution using the LM statistic. For the $Gamma(3, 1)$ distribution the results are similar. But, in all cases, the control chart with the LM statistic has a better performance than the LAB statistic. These results agreed with the work of Tercero-Gómez et al., 2020 where they showed that the Lepage-Mood statistic is a better alternative for most cases than the Lepage-Ansari-Bradley statistic for monitoring both the location and scale parameters of the process.

When Only Standard Deviation Changes

Now, figure 4.6 presents the Out-of-control performance of the proposed control chart for different shift sizes in scale and observations from the $N(0, 1)$ distribution. For condition i), and $m = 70$, we have an acceptable performance only when we consider a test sample size of $n = 25$; in this case, we see a $RSP_{50} \geq 0.95$ for $\tau \leq 0.5$ in both the alternatives (LM and LAB statistics). For $\tau \geq 1.5$, we have a $RSP_{50} \geq 0.85$ in this case for the control chart based on LM statistic, and this shows that the LM statistic has a better performance than using the LAB statistic instead. Only when $n = 10$, the LAB statistic has a better performance than the LM statistic when $\tau \leq 1.5^{-1}$, but this performance is not good. For condition ii) when the shift occurs after the middle of the production run, i.e., $c = 6$, the performance is similar; for $\tau \geq 2.0$ and $n = 25$, we see a $RSP_{50} \geq 0.90$ for the LM statistic. In this case, the control chart with LM statistic has a better performance than the LAB statistic. Figure 4.6 shows the performance for observations coming from a Student's $t(4)$ distribution, where we can see a pretty similar performance; again, the LM statistic presents, in general, a better performance than the LAB statistic. Only when $n = 25$, we obtain an acceptable performance in both the alternatives, for example, $RSP_{50} \geq 0.99$ when $\tau \leq 0.5$ and for $\tau \geq 2$, we have a $RSP_{50} \geq 0.8$ for LM statistic and condition i). When we consider condition ii), the performance remains at a reasonable level, when $\tau \leq 0.5$, the $RSP_{50} \geq 0.95$ for both the alternatives and when $\tau \geq 2$, we obtain a $RSP_{50} \geq 0.8$ for LM statistic that is a better performance than the LAB

statistic. Figures 4.8 and 4.9 presents the Out-of-control performance for observations coming from the asymmetrical distributions, $Gamma(2,1)$ and $Gamma(3,1)$. The LM statistic shows a better performance than the LAB statistic for most cases, but only when $n = 25$, that performance is robust, having a $RSP_{50} \geq 0.99$ for $\tau \leq 0.5$ and $RSP_{50} \geq 0.95$ when $\tau \geq 2$ for observations with a $Gamma(2,1)$ distribution and condition i). Finally, when we consider observations from the $Gamma(3,1)$ distribution, the performance is similar, for $\tau \geq 2$, we have a $RSP_{50} \geq 0.9$ using the LM statistic and a test sample size of 25 and condition i), for condition ii), the performance is also acceptable for both distributions having a $RSP_{50} \geq 0.85$ for $\tau \geq 2$. Finally, for shift sizes $\tau \leq 1.5^{-1}$ the LAB statistic performs better than the LM statistic, but this performance is not robust in these cases. For $n = 25$, the OOC performance of the control chart is robust for both the alternatives and over these scenarios the LM statistic presents better performance than the LAB statistic.

When both mean and Standard deviation Changes

We considered the following scale and location shift sizes for each considered distribution in subsection 4.2.2 to generate our plot for this subsection:

- Scale shift size $\tau = \{0.5, 1.5^{-1}, 1.5\}$
- Location shift size $\delta = \{0, 0.25, 0.5, 0.75, 1, 1.5, 2\}$

Figure 4.10 shows the trend of $RSP_{50}(c, I)$-(y-axis) over the location shift size δ-(x-axis) for $N(0,1)$ distribution and $\tau = 0.5$. Considering the LM statistic we have an acceptable performance of the control chart, for example, when $m = 30$ we obtain a $RSP_{50}(c, I) \geq 0.85$ for $\delta \geq 1.0$ and condition i); when $m = 70$, the $RSP_{50}(c, I) \geq 0.99$ for $\delta \geq 1.0$ and condition i), for condition ii) we have $RSP_{50}(c, I) \geq 0.95$ for $\delta \geq 1.0$. As we can see in the values of $RSP_{50}(c, I)$ the LM statistic outperformed the LAB statistic for these scenarios. In figure 4.11 where $\tau = 1.5^{-1}$ we obtain an acceptable performance only for $m = 70$ and condition i) with the LM statistic, where wwe have an $RSP_{50}(c, I) \geq 0.99$ for $\delta \geq 1.0$. Similar results are found in figure 4.12 where $\tau = 1.5$.

Figures 4.13, 4.14 and 4.15 illustrate the behavior of $RSP_{50}(c, I)$ for Student's $t(4)$ distribution. In figure 4.13 where $\tau = 0.5$, we have an acceptable performance in all cases considering the LM statistic; for example, for condition i) and $m = 30$, we obtain an $RSP_{50}(c, I) \geq 0.99$ for $\delta \geq 1.0$ and for $m = 70$ we have an $RSP_{50}(c, I) \geq 0.90$ for $\delta \geq 0.75$. We obtain similar values of $RSP_{50}(c, I)$ when considering condition ii). Only for $m = 30$ the LM statistic shows a better performance than the LAB statistic, in the rest of the cases

the peformance is quite similar. Analogous results for LM and LAB statistics are found in figure 4.14. In figure 4.15 the difference between the LM and LAB statistic is more remarkable, for example, considering condition ii) and $m = 70$, the $RSP_{50}(c, I) \geq 0.63$ for $\delta \geq 1.0$ with LAB statistic, conversely, $RSP_{50}(c, I) \geq 0.97$ for $\delta \geq 1.0$ for LM statistic with the same settings. The control chart presents a robust performance with the LM statistic for condition i) and $m = 70$ having an $RSP_{50}(c, I) \geq 0.95$ for $\delta \geq 0.75$.

Figures 4.16, 4.17 and 4.18 show the trend of $RSP_{50}(c, I)$ for observations coming from the $Gamma(2, 1)$ distribution. In figure 4.16 where $\tau = 0.5$ we obtain a robust performance for both the alternatives LM and LAB statistic having an $RSP_{50}(c, I) \geq 0.99$ for $\delta \geq 0.5$ considering both conditions i) and ii) and a test sample size $n = 25$. When we consider $n = 10$, we have an acceptable performance only for the LM statistic showing an $RSP_{50}(c, I) \geq 0.99$ for $\delta \geq 1.0$ in both conditions i) and ii). Similar results are found in figure 4.17. In figure 4.18 for $tau = 1.5$ the control chart is less sensitive, only for $n = 25$ we have a robust performance for both the alternatives LM and LAB statistic with an $RSP_{50}(c, I) \geq 0.99$ for $\delta \geq 0.5$.

Figures 4.19, 4.20 and 4.21 present the results for the $Gamma(3, 1)$ distribution. In figures 4.19 and 4.20 where $\tau = 0.5$ and $\tau = 1.5^{-1}$ respectively, we have a robust performance when $n = 25$ having an $RSP_{50}(c, I) \geq 0.99$ for $\delta \geq 0.5$ with both the alternatives LM and LAB statistics and both conditions i) and ii). For $n = 10$ the LM statistic shows a better performance than the LAB statistic and it shows an acceptable performance having an $RSP_{50}(c, I) \geq 0.99$ for $\delta \geq 1.0$ in both conditions i and ii). Finally, in figure 4.21 the control chart is less sensitive, only when we consider $n = 25$ we obtain a robust performance of the control chart with an $RSP_{50}(c, I) \geq 0.99$ for $\delta \geq 0.5$ for both conditions i) and ii). In general, we see that the control chart needs a reference sample size of at least $m = 70$ and a test sample size of $n = 25$ to show a robust OOC performance.

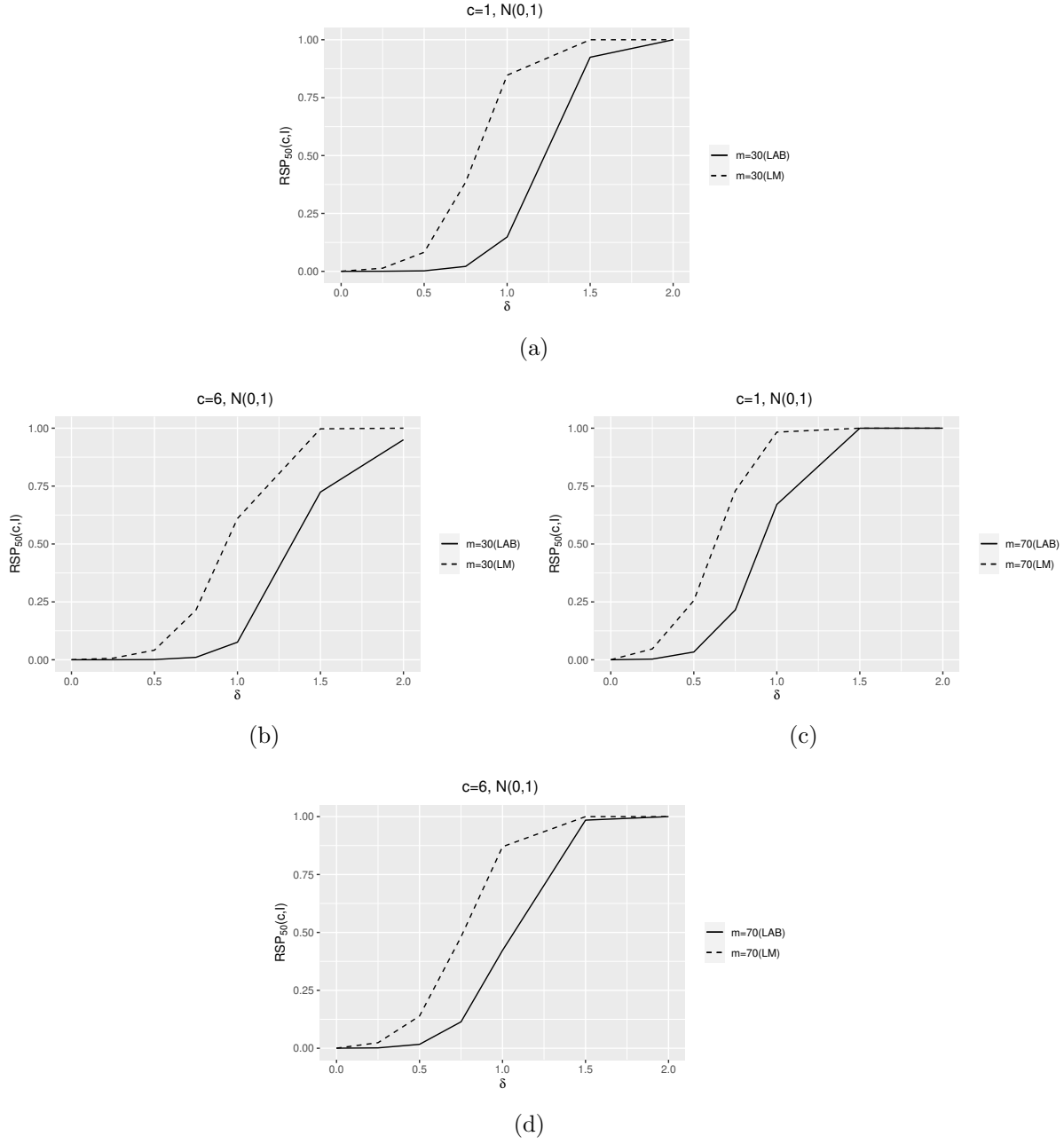

Figure 4.2: $N(0,1)$. Out-of-control performance for shifts in location. Lot dimension $L = 1000$, $FAP_0 = 0.1$, $I = 10$ inspections, reference sample size $m = \{30, 70\}$, test sample size $n = 10$, $c = \{1, 6\}$.

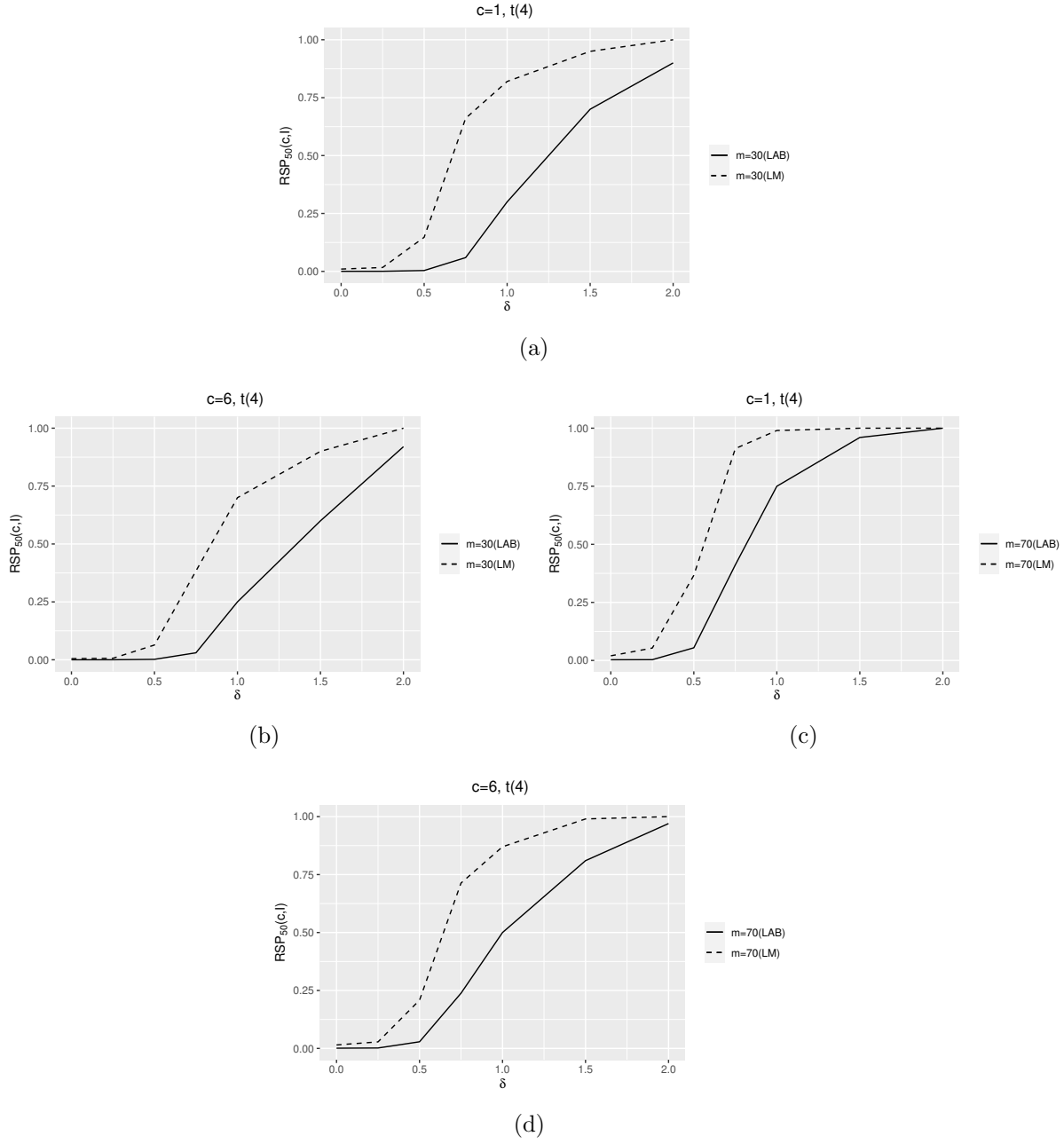

Figure 4.3: $t(4)$. Out-of-control performance for shifts in location. Lot dimension $L = 1000$, $FAP_0 = 0.1$, $I = 10$ inspections, reference sample size $m = \{30, 70\}$, test sample size $n = 10$, $c = \{1, 6\}$.

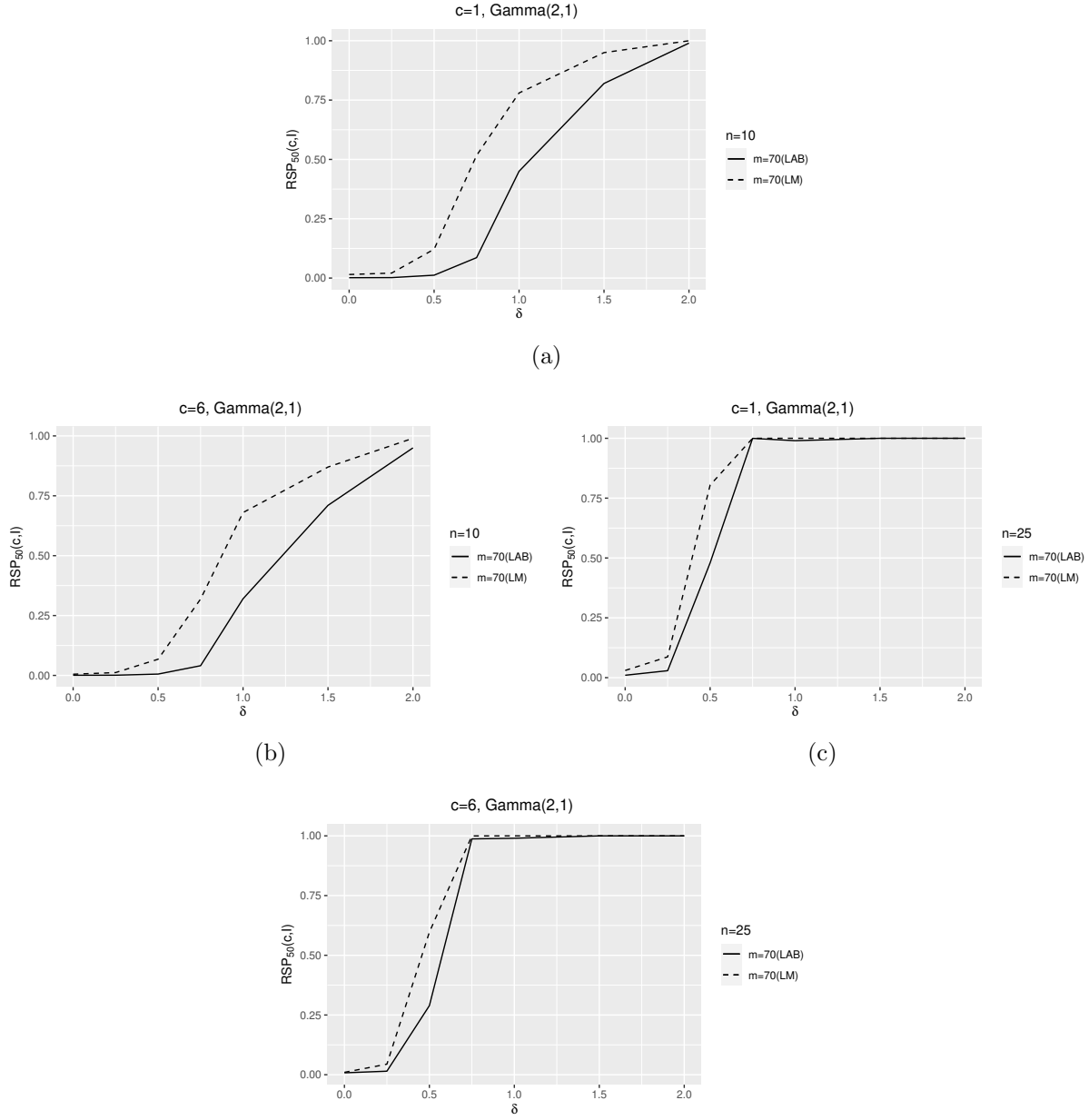

Figure 4.4: $Gamma(2,1)$. Out-of-control performance for shifts in location. Lot dimension $L = 1000$, $FAP_0 = 0.1$, $I = 10$ inspections, reference sample size $m = \{70\}$, test sample size $n = \{10, 25\}$, $c = \{1, 6\}$.

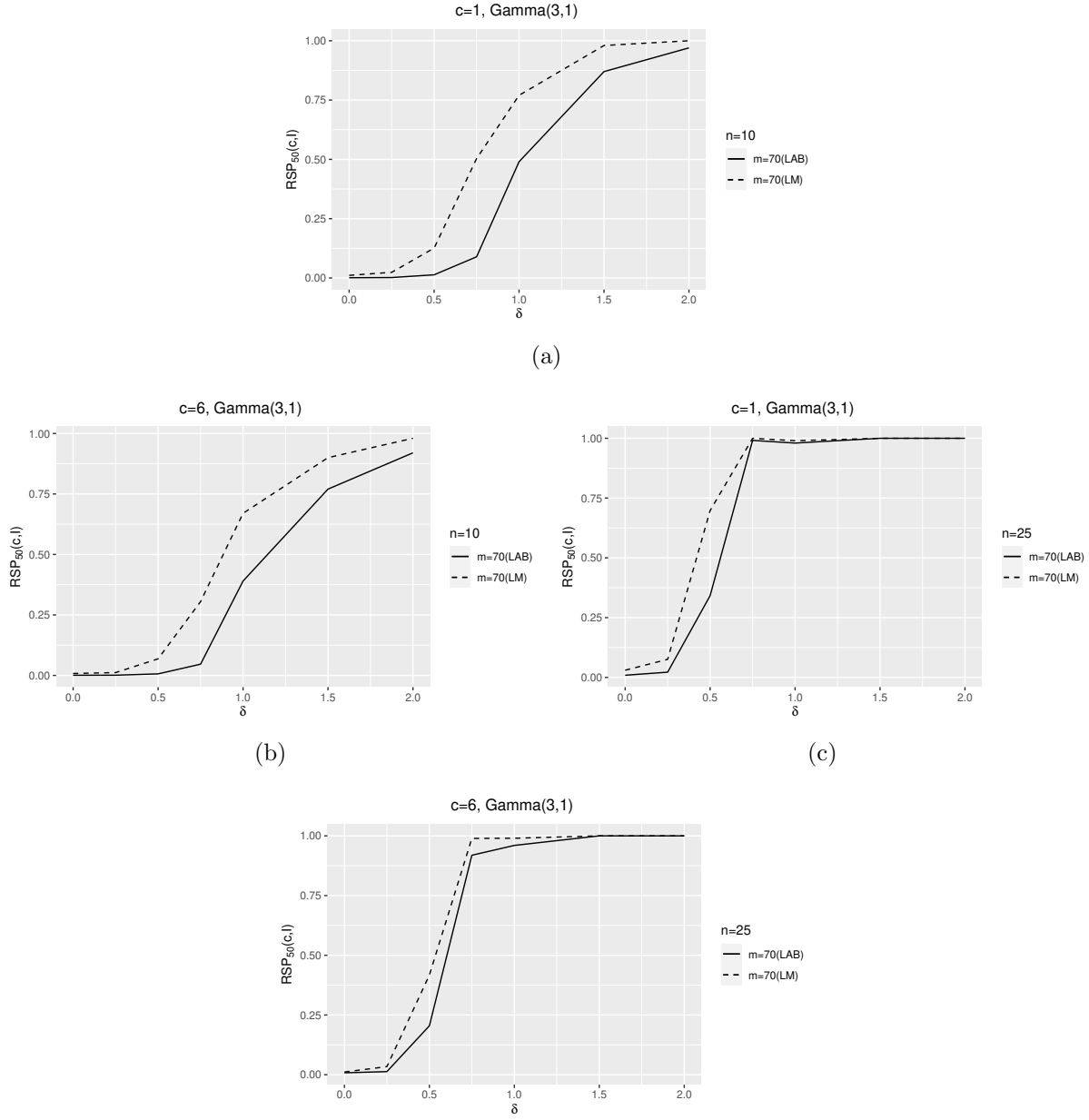

Figure 4.5: $Gamma(3,1)$. Out-of-control performance for shifts in location. Lot dimension $L = 1000$, $FAP_0 = 0.1$, $I = 10$ inspections, reference sample size $m = \{70\}$, test sample size $n = \{10, 25\}$, $c = \{1, 6\}$.

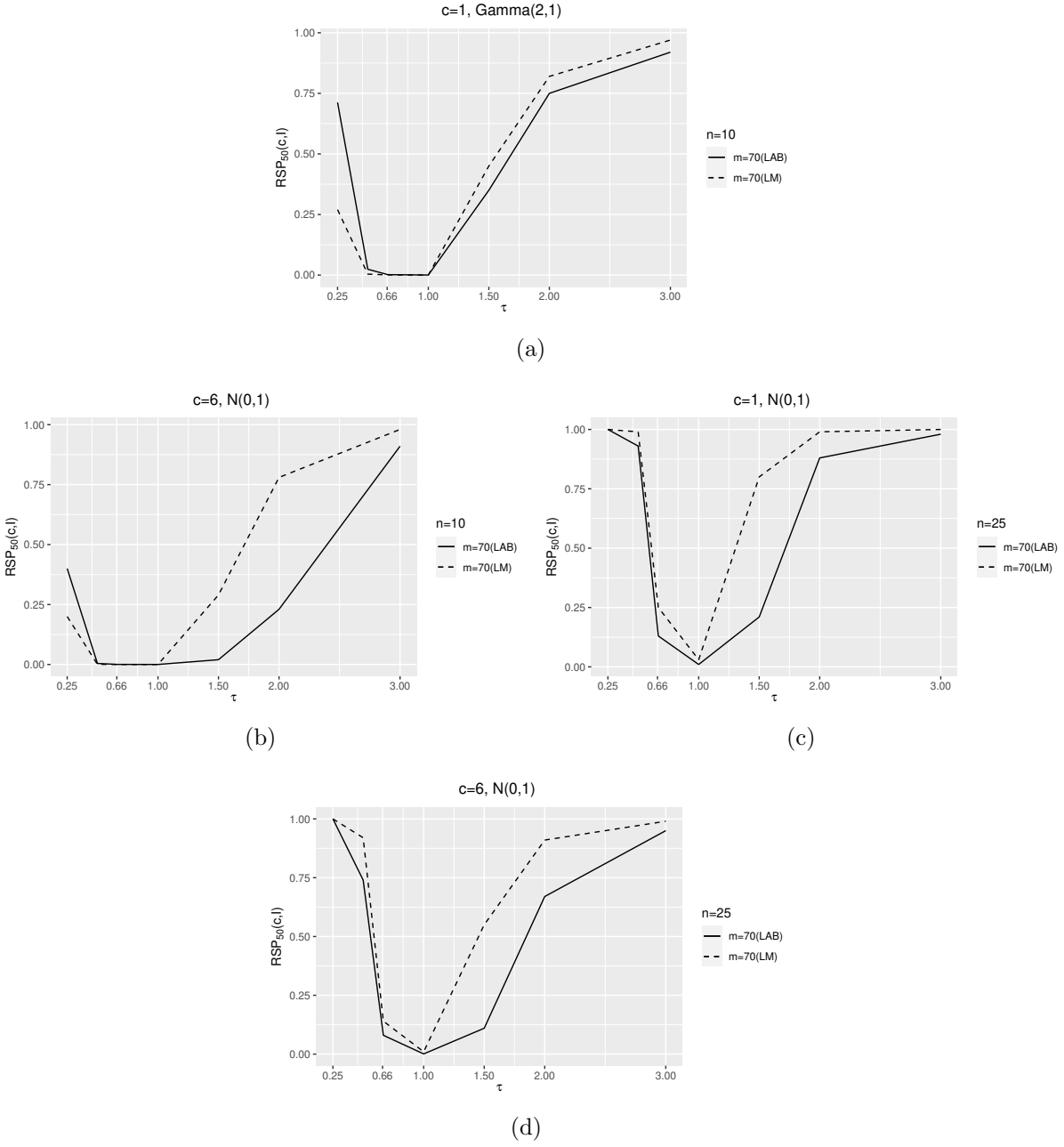

Figure 4.6: $N(0,1)$. Out-of-control performance for shifts in scale. Lot dimension $L = 1000$, $FAP_0 = 0.1$, $I = 10$ inspections, reference sample size $m = \{70\}$, test sample size $n = \{10, 25\}$, $c = \{1, 6\}$.

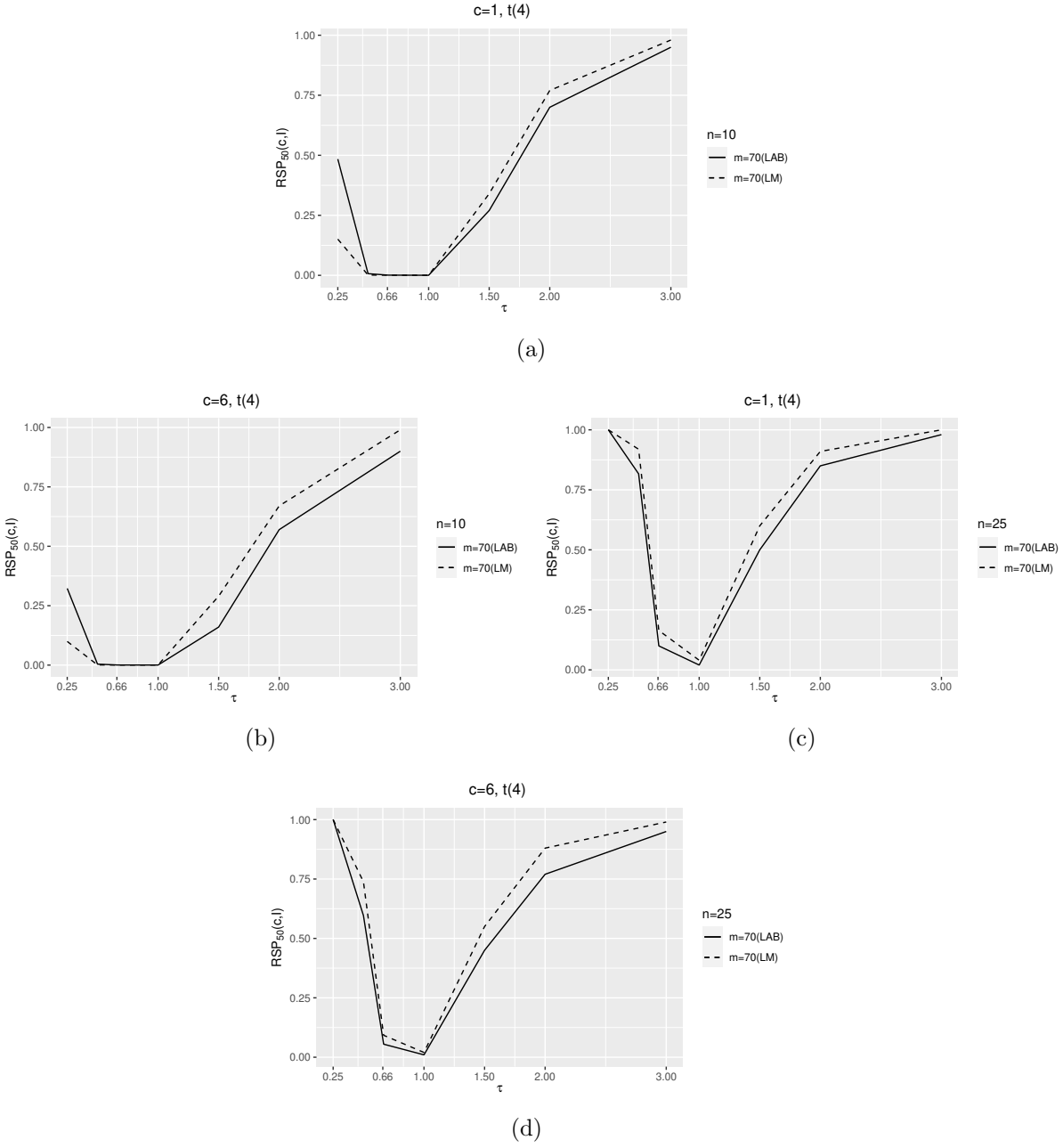

Figure 4.7: $t(4)$. Out-of-control performance for shifts in scale. Lot dimension $L = 1000$, $FAP_0 = 0.1$, $I = 10$ inspections, reference sample size $m = \{70\}$, test sample size $n = \{10, 25\}$, $c = \{1, 6\}$.

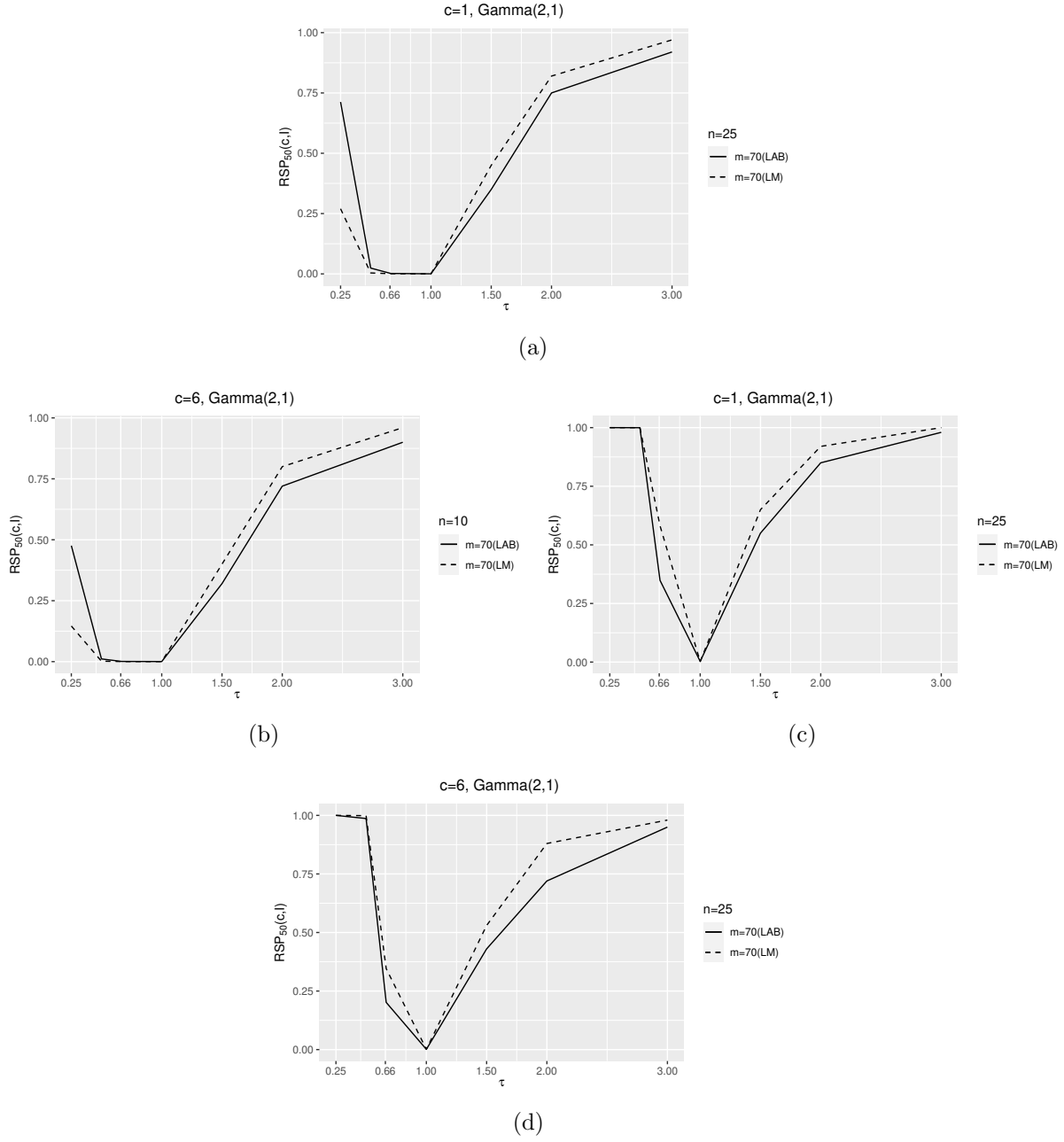

Figure 4.8: $Gamma(2,1)$. Out-of-control performance for shifts in scale. Lot dimension $L = 1000$, $FAP_0 = 0.1$, $I = 10$ inspections, reference sample size $m = \{70\}$, test sample size $n = \{10, 25\}$, $c = \{1, 6\}$.

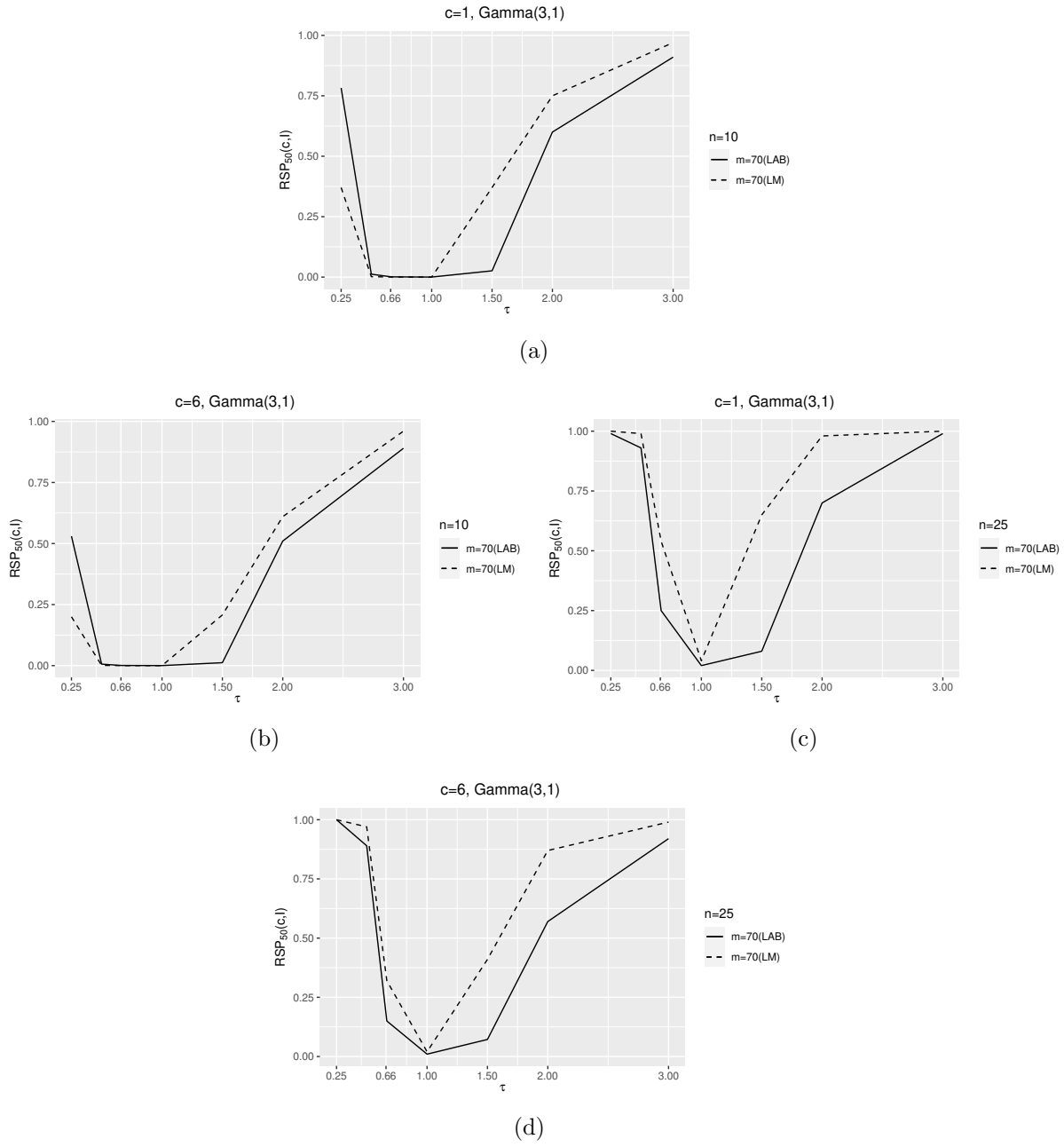

Figure 4.9: $Gamma(3,1)$. Out-of-control performance for shifts in scale. Lot dimension $L = 1000$, $FAP_0 = 0.1$, $I = 10$ inspections, reference sample size $m = \{70\}$, test sample size $n = \{10, 25\}$, $c = \{1, 6\}$.

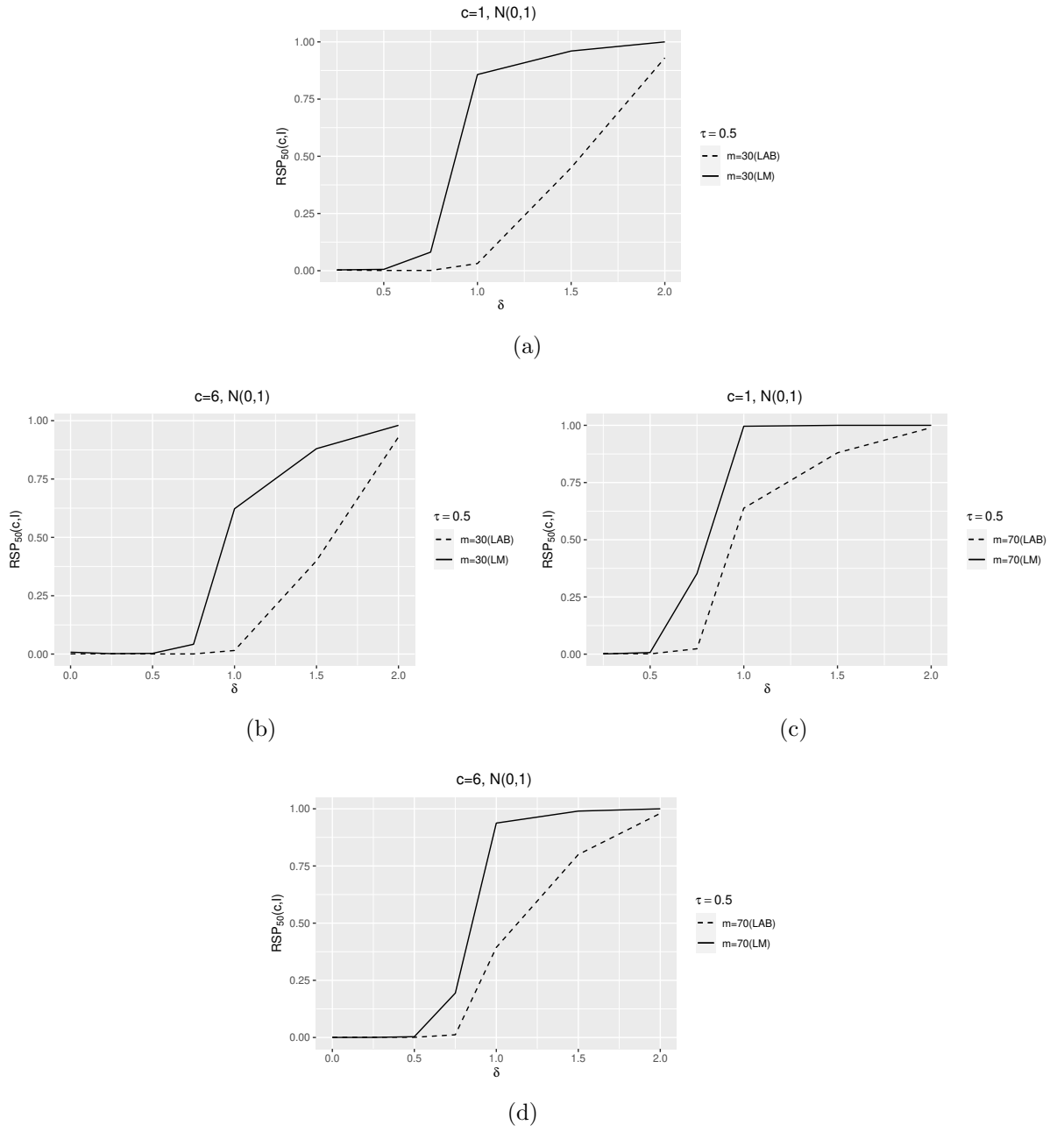

Figure 4.10: $N(0,1)$, $\tau = 0.5$. Out-of-control performance for shifts in location and scale. Lot dimension $L = 1000$, $FAP_0 = 0.1$, $I = 10$ inspections, reference sample size $m = \{30, 70\}$, test sample size $n = \{10\}$, $c = \{1, 6\}$.

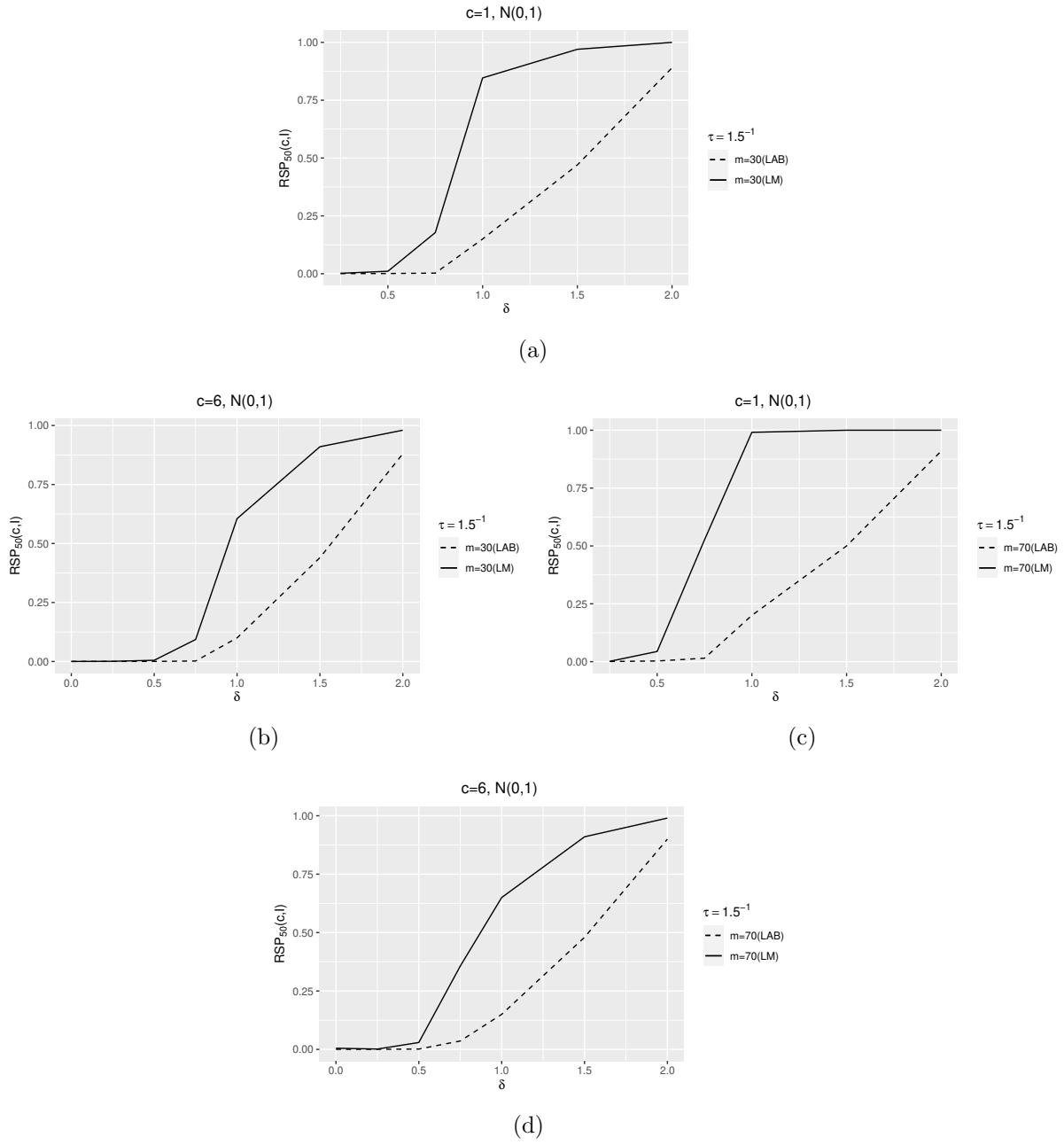

Figure 4.11: $N(0,1)$, $\tau = 1.5^{-1}$. Out-of-control performance for shifts in location and scale. Lot dimension $L = 1000$, $FAP_0 = 0.1$, $I = 10$ inspections, reference sample size $m = \{30, 70\}$, test sample size $n = \{10\}$, $c = \{1, 6\}$.

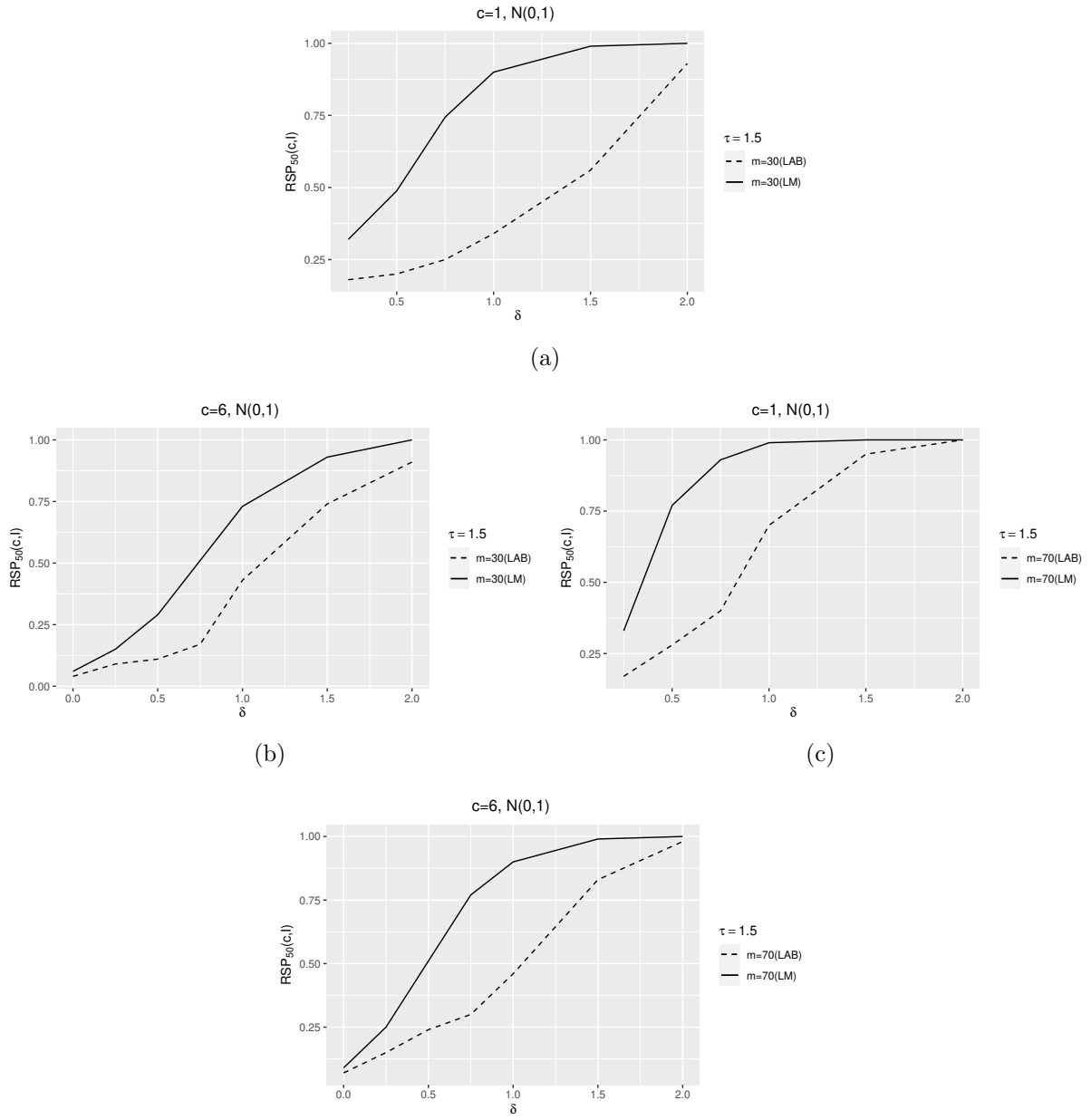

Figure 4.12: $N(0,1)$, $\tau = 1.5$. Out-of-control performance for shifts in location and scale. Lot dimension $L = 1000$, $FAP_0 = 0.1$, $I = 10$ inspections, reference sample size $m = \{30, 70\}$, test sample size $n = \{10\}$, $c = \{1, 6\}$.

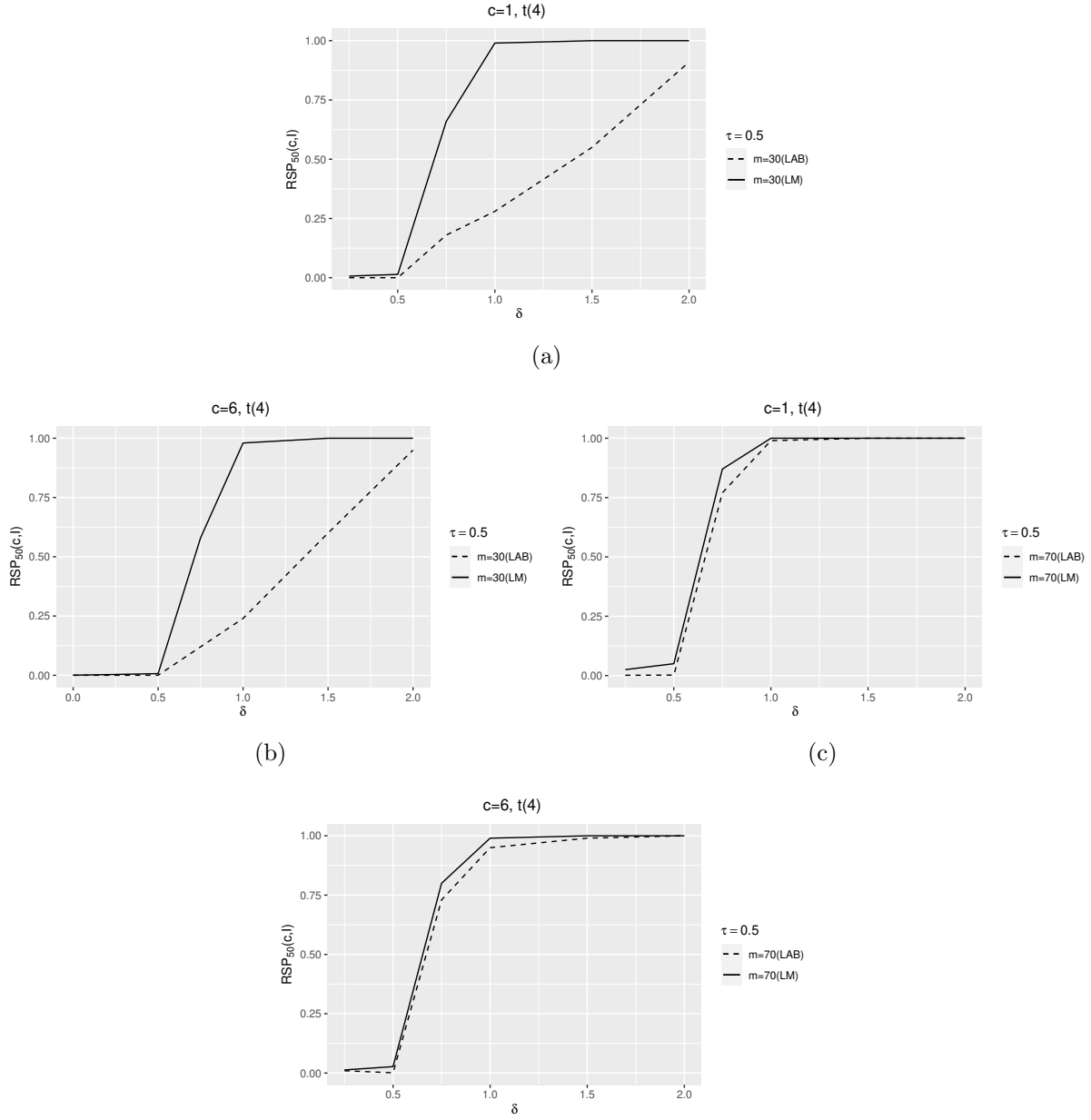

Figure 4.13: $t(4)$, $\tau = 0.5$. Out-of-control performance for shifts in location and scale. Lot dimension $L = 1000$, $FAP_0 = 0.1$, $I = 10$ inspections, reference sample size $m = \{30, 70\}$, test sample size $n = \{10\}$, $c = \{1, 6\}$.

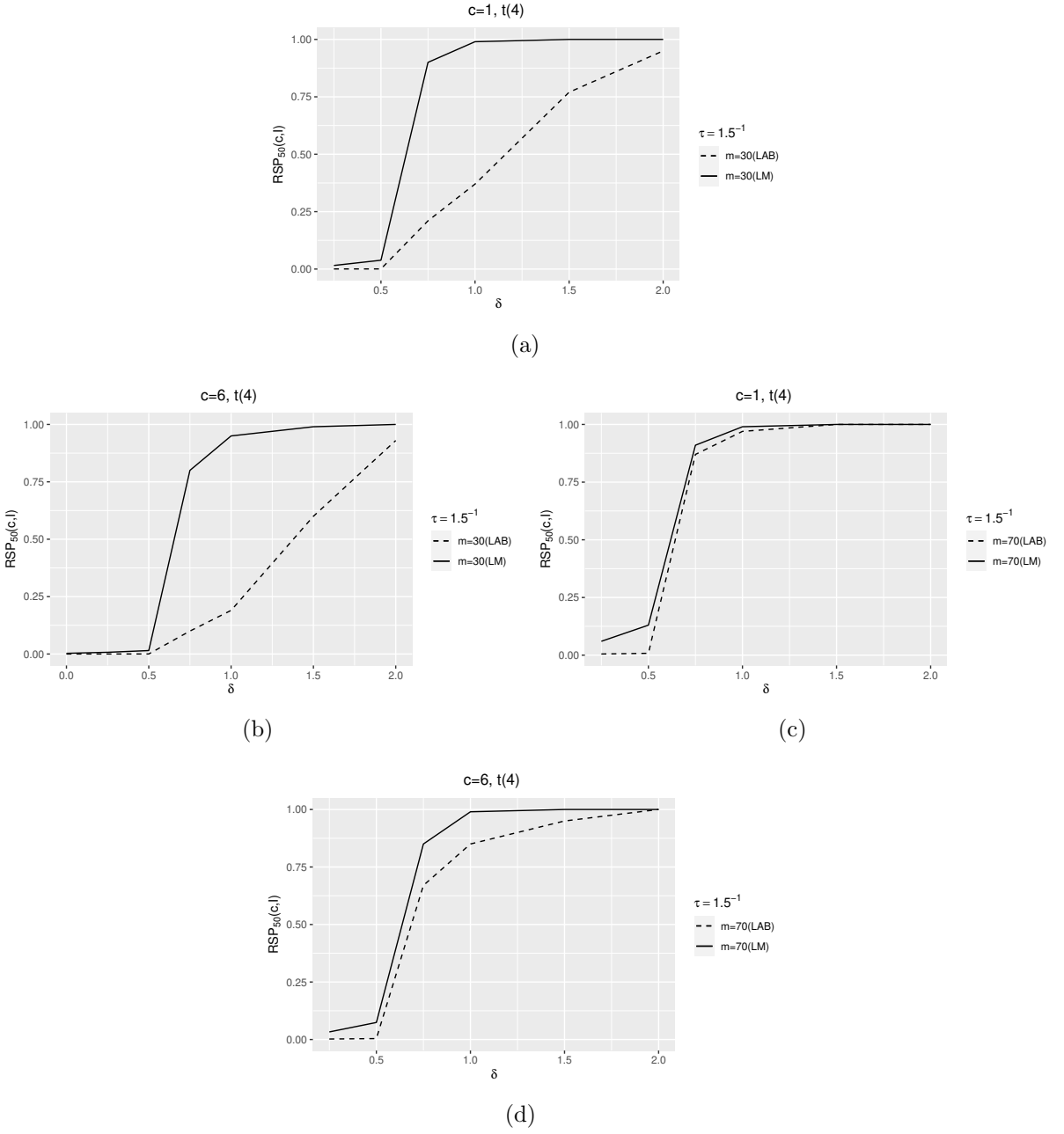

Figure 4.14: $t(4)$, $\tau = 1.5^{-1}$. Out-of-control performance for shifts in location and scale. Lot dimension $L = 1000$, $FAP_0 = 0.1$, $I = 10$ inspections, reference sample size $m = \{30, 70\}$, test sample size $n = \{10\}$, $c = \{1, 6\}$.

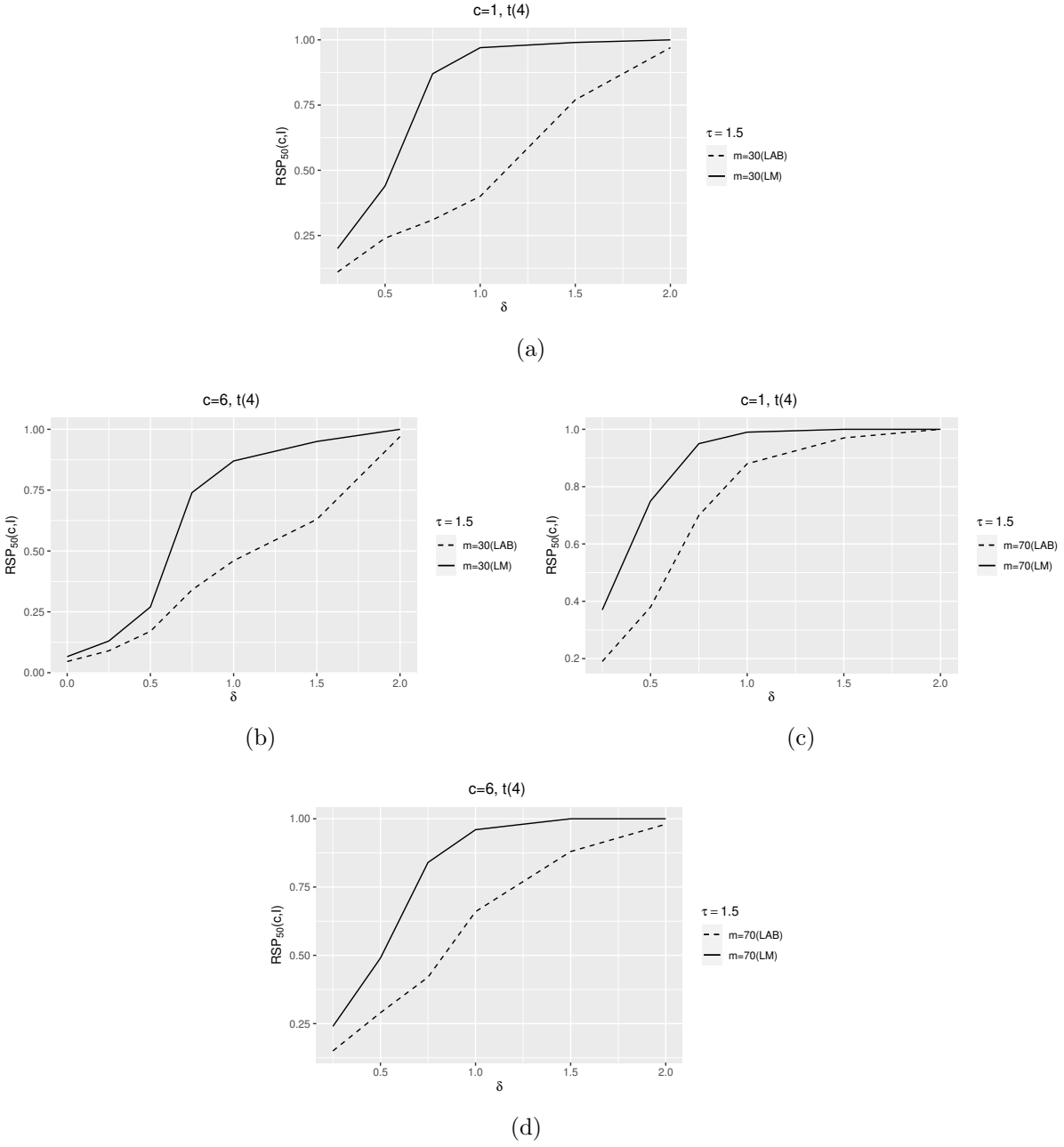

Figure 4.15: $t(4)$, $\tau = 1.5$. Out-of-control performance for shifts in location and scale. Lot dimension $L = 1000$, $FAP_0 = 0.1$, $I = 10$ inspections, reference sample size $m = \{30, 70\}$, test sample size $n = \{10\}$, $c = \{1, 6\}$.

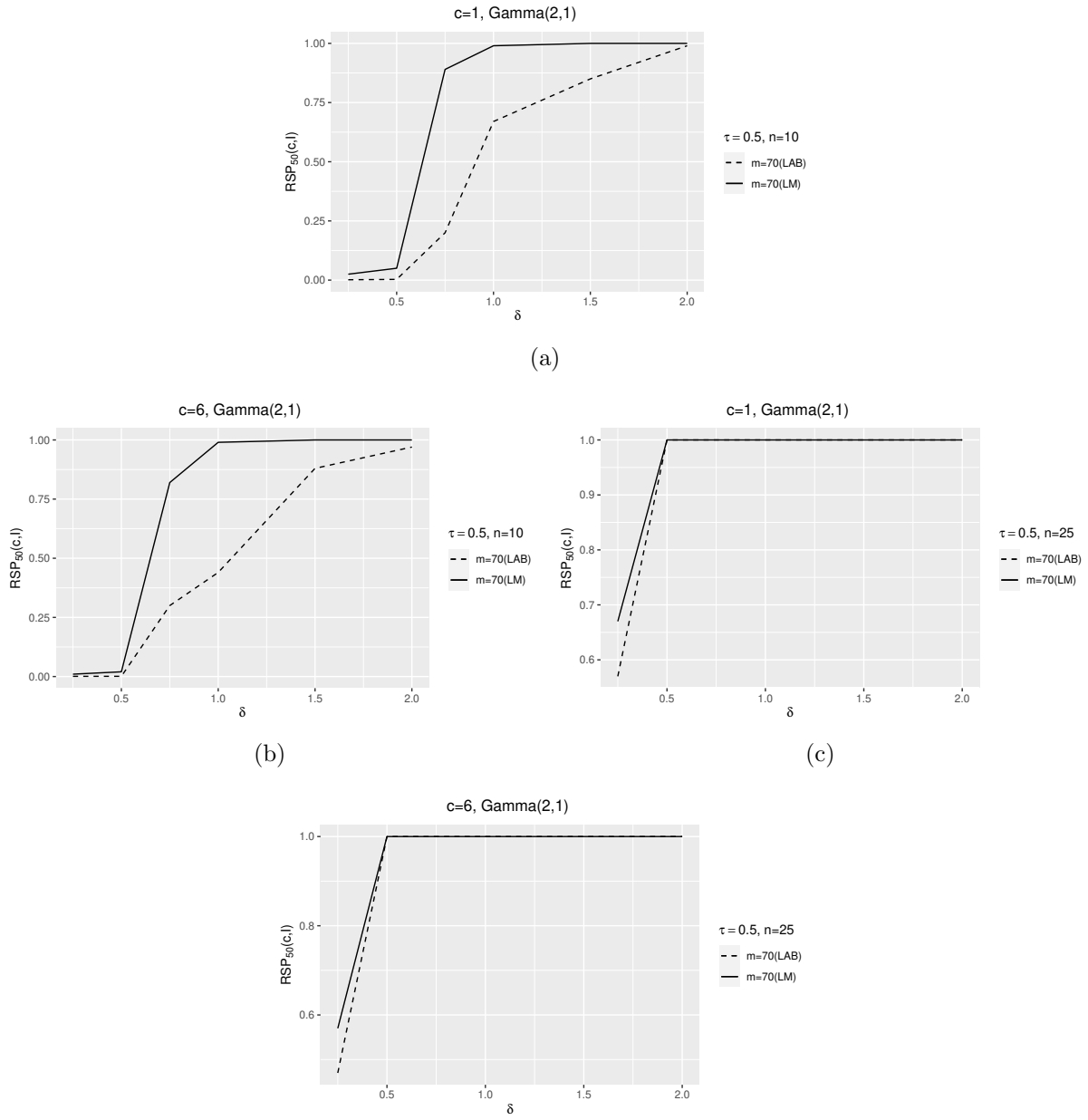

Figure 4.16: $Gamma(2,1)$, $\tau = 0.5$. Out-of-control performance for shifts in location and scale. Lot dimension $L = 1000$, $FAP_0 = 0.1$, $I = 10$ inspections, reference sample size $m = \{70\}$, test sample size $n = \{10, 25\}$, $c = \{1, 6\}$.

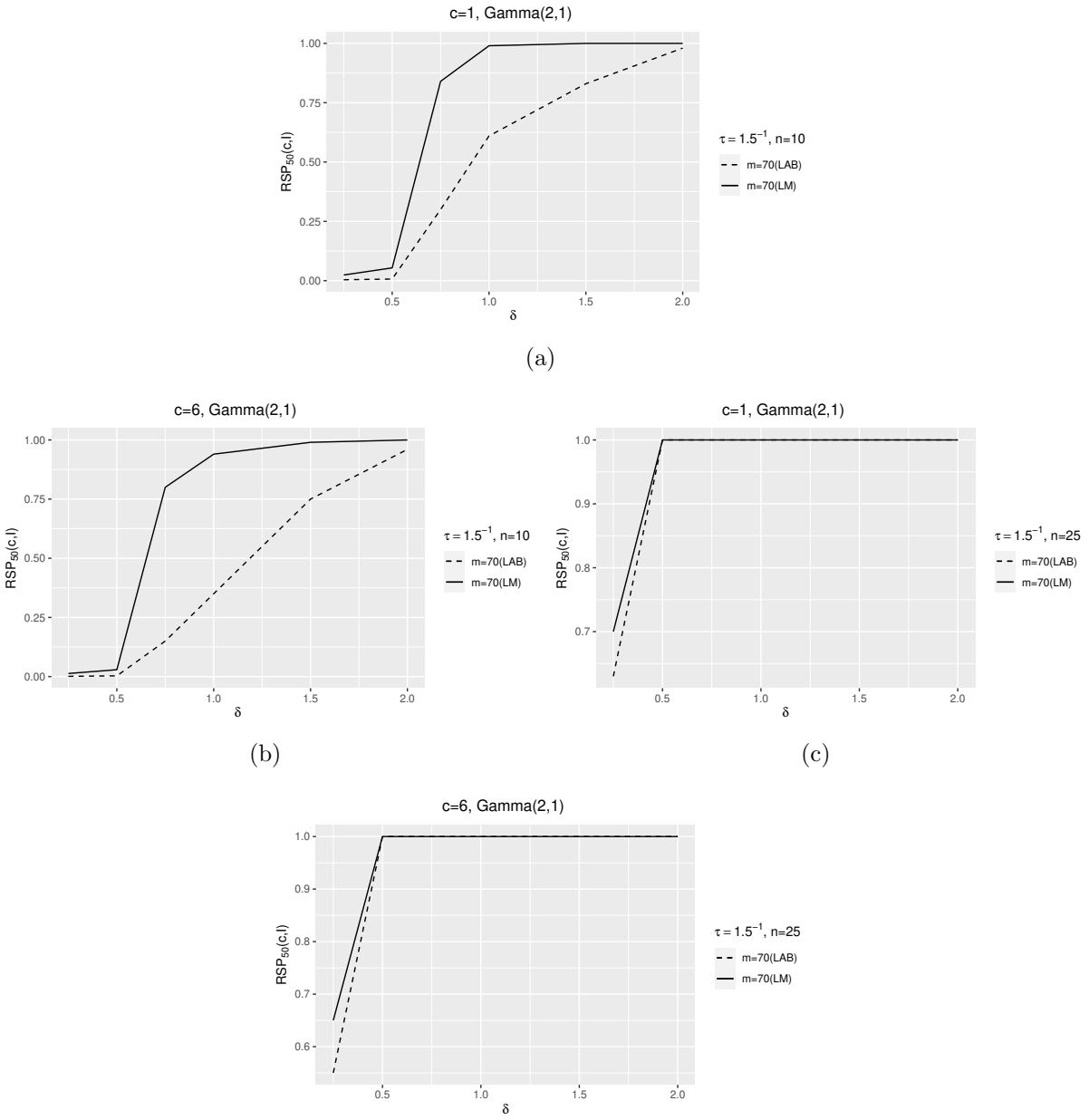

Figure 4.17: $Gamma(2,1)$, $\tau = 1.5^{-1}$. Out-of-control performance for shifts in location and scale. Lot dimension $L = 1000$, $FAP_0 = 0.1$, $I = 10$ inspections, reference sample size $m = \{70\}$, test sample size $n = \{10, 25\}$, $c = \{1, 6\}$.

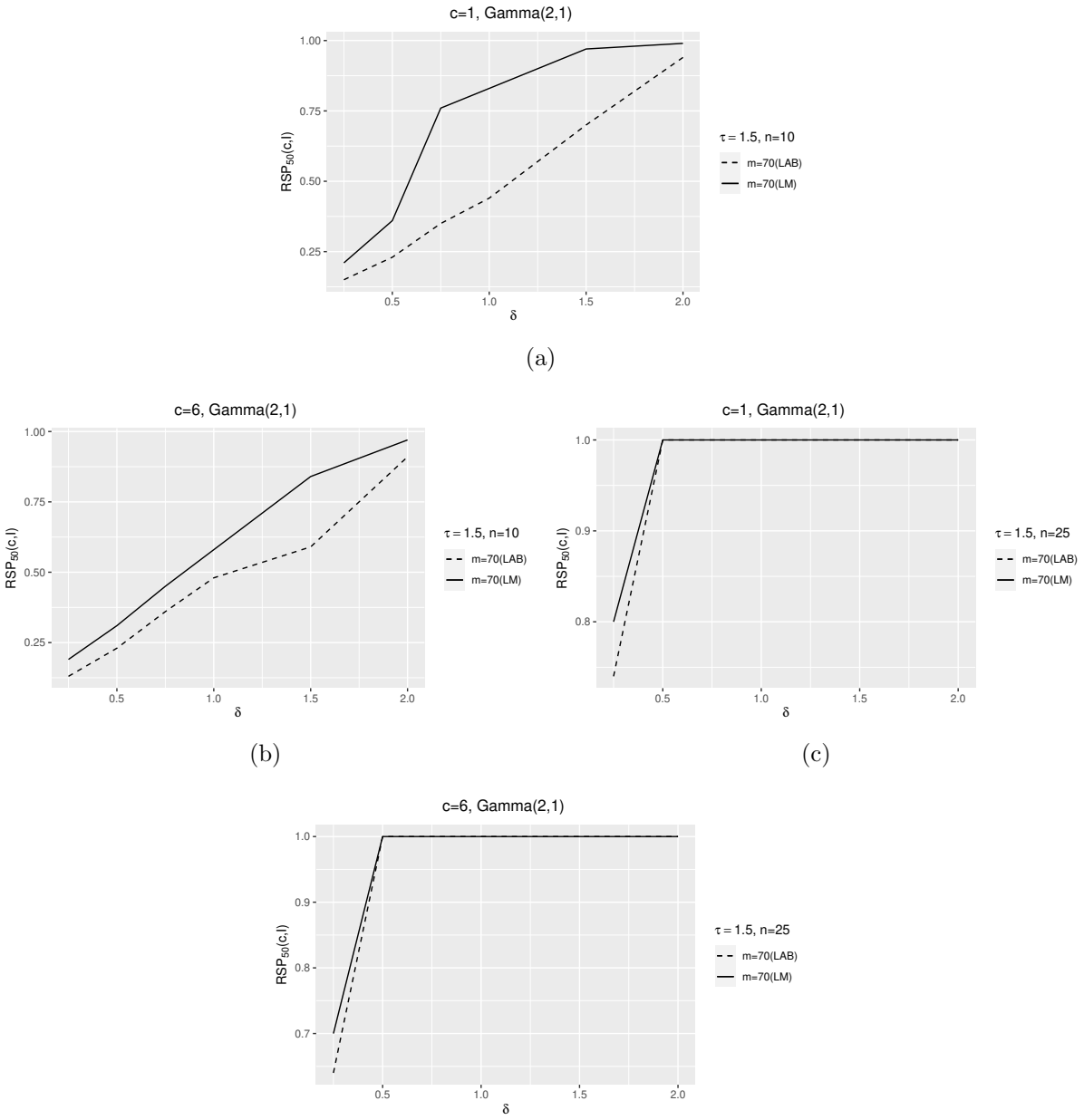

Figure 4.18: $Gamma(2,1)$, $\tau = 1.5$. Out-of-control performance for shifts in location and scale. Lot dimension $L = 1000$, $FAP_0 = 0.1$, $I = 10$ inspections, reference sample size $m = \{70\}$, test sample size $n = \{10, 25\}$, $c = \{1, 6\}$.

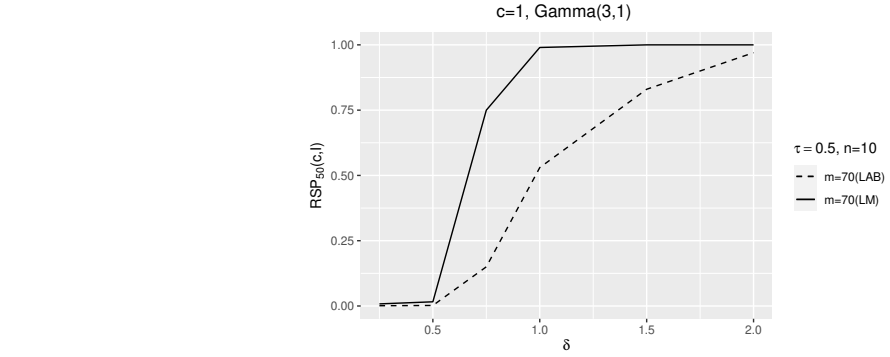

(a)

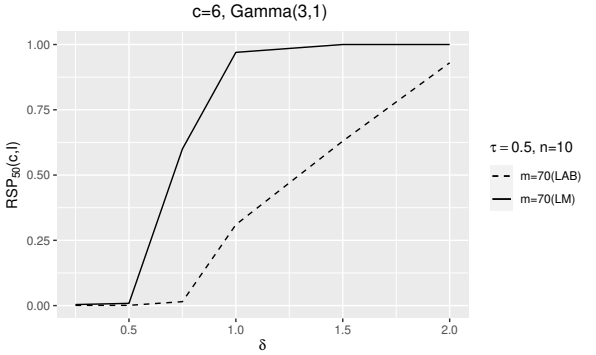

(b)

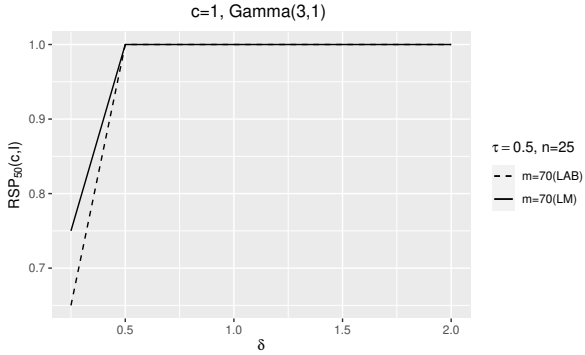

(c)

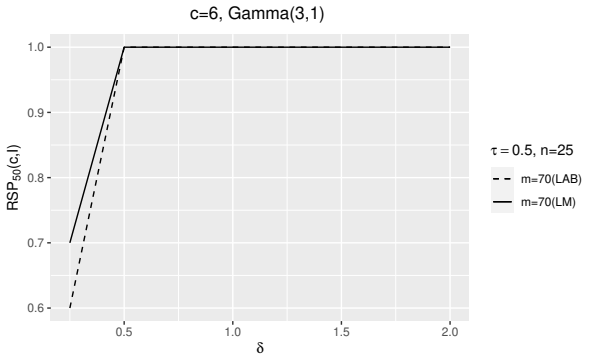

(d)

Figure 4.19: $Gamma(3,1)$, $\tau = 0.5$. Out-of-control performance for shifts in location and scale. Lot dimension $L = 1000$, $FAP_0 = 0.1$, $I = 10$ inspections, reference sample size $m = \{70\}$, test sample size $n = \{10, 25\}$, $c = \{1, 6\}$.

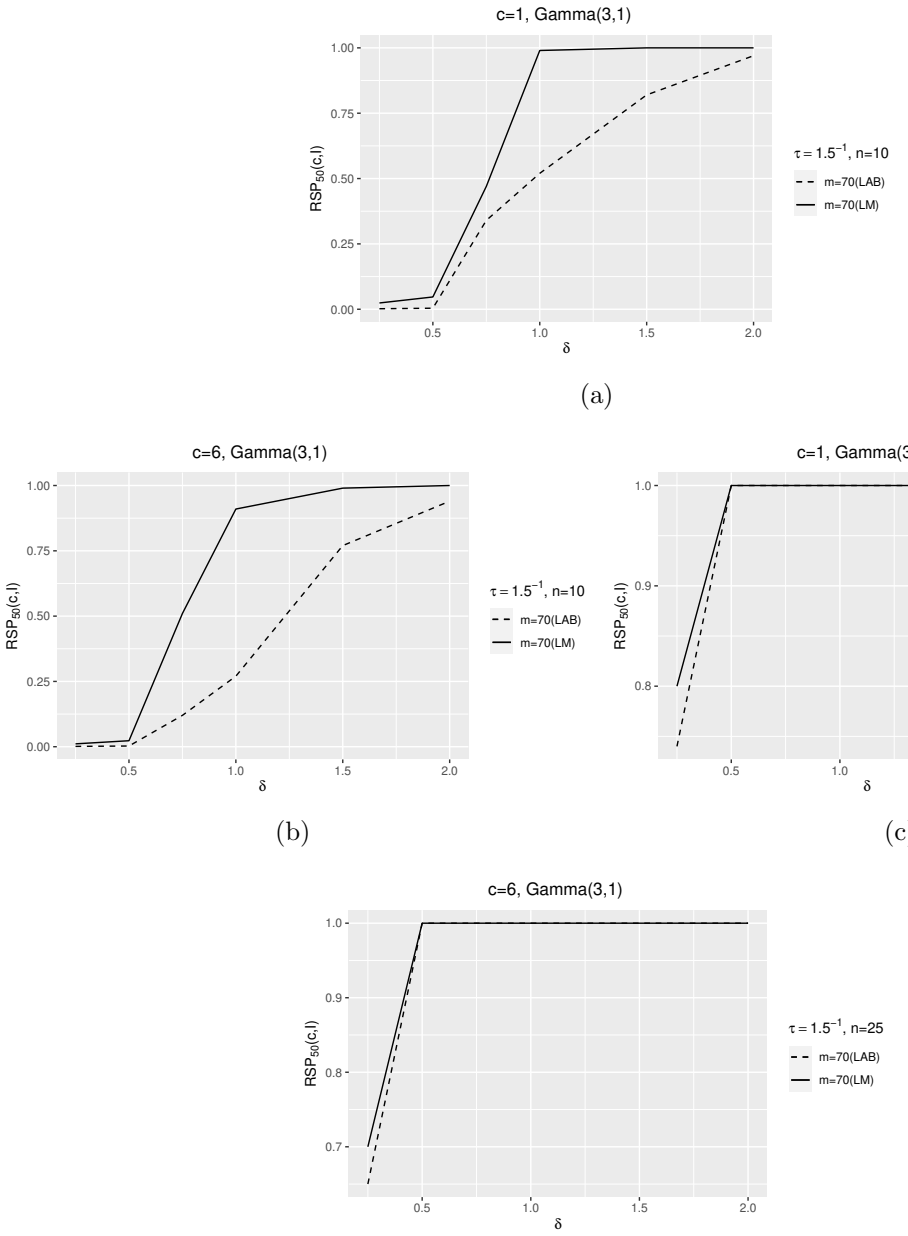

Figure 4.20: $Gamma(3,1)$, $\tau = 1.5^{-1}$. Out-of-control performance for shifts in location and scale. Lot dimension $L = 1000$, $FAP_0 = 0.1$, $I = 10$ inspections, reference sample size $m = \{70\}$, test sample size $n = \{10, 25\}$, $c = \{1, 6\}$.

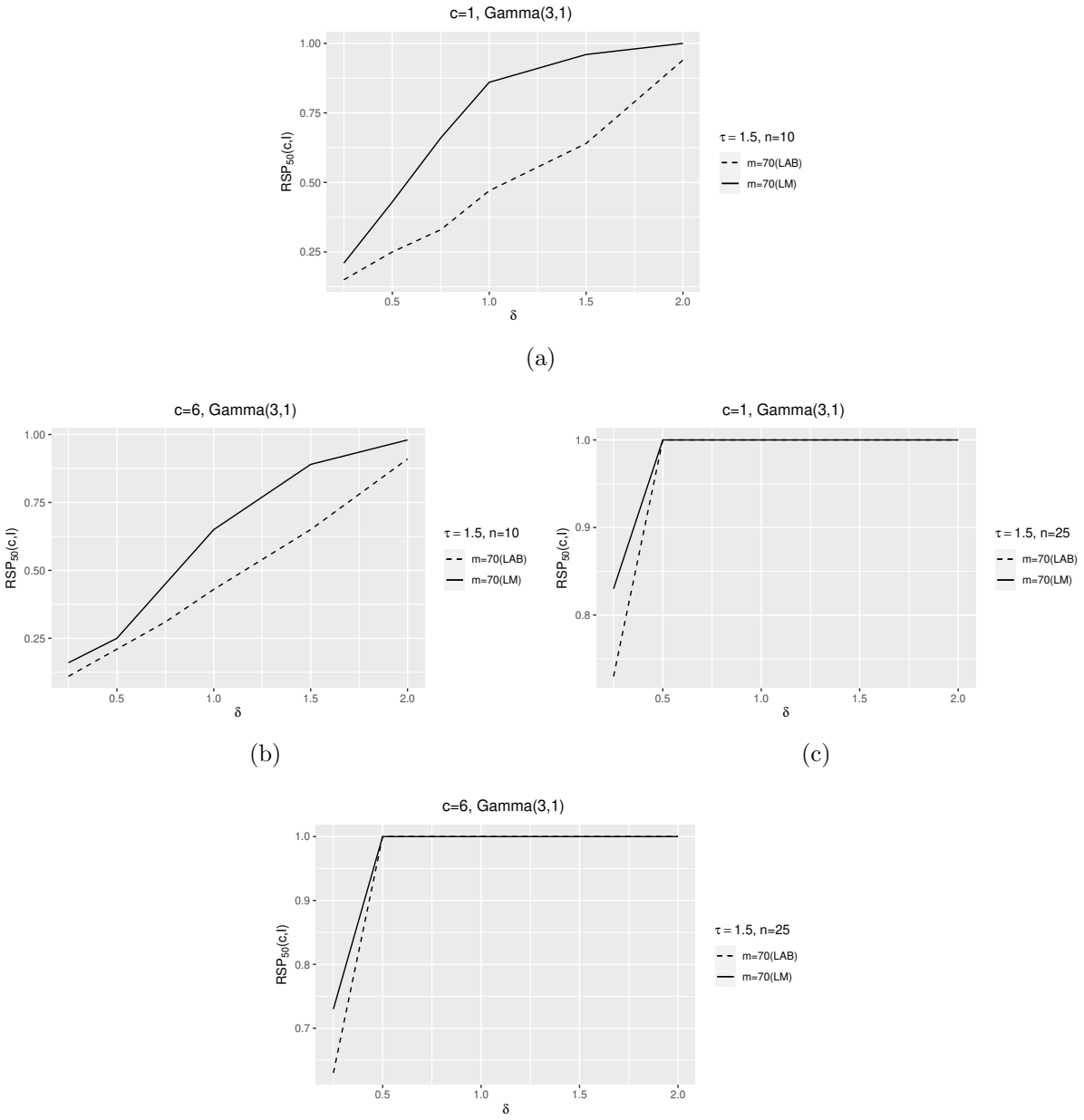

Figure 4.21: $Gamma(3,1)$, $\tau = 1.5$. Out-of-control performance for shifts in location and scale. Lot dimension $L = 1000$, $FAP_0 = 0.1$, $I = 10$ inspections, reference sample size $m = \{70\}$, test sample size $n = \{10, 25\}$, $c = \{1, 6\}$.

Chapter 5
Conclusions

5.1 Conclusions

In this study, a Shewhart-type control chart for joint monitoring of location and scale parameters for finite horizon production processes based on the Lepage-Mood(LM) statistic was proposed, taking into account the practitioner-to-practitioner variability. Online monitoring of Finite Horizon Production (FHP) processes is a challenging task for practitioners and there is a need for developing statistical tools for online monitoring of this kind of processes. We evaluated the conditional performance of our proposed control chart to generate guaranteed control limits that lead us to the desired performance of the control chart in the In-control state of the process. With these control limits, the practitioners know the probability of having a false alarm larger than a predefined target. By this reason the proposed control chart with the conditional scheme is a better alternative than the common unconditional scheme for the In-control analysis in terms of a guaranteed performance of the control chart.

The simulations results shows that even the control limits are wider, the control chart shows a good power to detect medium or large changes in the process. Small changes are not easily detected by this control chart, which is a common result for Shewhart control charts. The comparison of the proposed control chart with Lepage-Mood statistic versus the use of the classical Lepage statistic (with Ansary-Bradley statistic) shows a better performance for detecting changes in our proposed control chart. These results agree the reported in Tercero-Gómez et al., 2020 for infinite processes.

5.2 Future Work

In this work, we proposed a nonparametric control chart for univariate finite horizon production processes(FHP). However, there is the need to develop a control chart for the multivariate case of finite-horizon production processes, as was mentioned in Celano

and Chakraborti, 2020. Nonparametric statistics can be used combined with distances measures to convert multivariate observations in univariate statistics, as it was done in Mukherjee and Marozzi, 2020.

Also, in order to detect small changes combined with the conditional scheme, we can analyze other control charts, like EWMA or CUSUM, see Celano et al., 2015 and Nenes and Tagaras, 2010. Also, implementing a Markov-Chain approach could improve the performance of a control chart for FHP processes. On the other hand, an economic design of a control chart for an FHP process, see Nenes et al., 2017, where the conditional performance is evaluated, might be an interesting topic of research to assess the economic implications of this conditional approach.

Bibliography

Albers, W., & Kallenberg, W. C. M. (2005). New corrections for old control charts. *Quality Engineering*, 467–473.

Albers, W., Kallenberg, W. C., & Nurdiati, S. (2005). Exceedance probabilities for parametric control charts. *Statistics*, 429–443.

Capizzi, G., & Masarotto, G. (2020). Guaranteed in-control control chart performance with cautious parameter learning. *Journal of Quality Technology*.

Celano, G., & Castagliola, P. (2018a). An EWMA Sign Control Chart with Varying Control Limits for Finite Horizon Processes. *Quality and Reliability Engineering Internationa*.

Celano, G., & Castagliola, P. (2018b). The Shewhart F control chart for monitoring processes with finite number of inspections. *Quality and Reliability Engineering International*.

Celano, G., Castagliola, P., & Chakraborti, S. (2016). Joint Shewhart Control Charts for Location and Scale Monitoring in Finite Horizon Processes. *Computers and Industrial Engineering*.

Celano, G., Castagliola, P., Chakraborti, S., & Nenes, G. (2015). The Performance of the Shewhart Sign Control Chart for Finite Horizon Processes. *The International Journal of Advanced Manufacturing Technology*.

Celano, G., Castagliola, P., Sergio, F., & Enrico, T. (2011). Shewhart and ewma t control charts for short production runs. *Quality and Reliability Engineering International*.

Celano, G., & Chakraborti, S. (2020). A distribution-free Shewhart-type Mann-Whitney control chart for monitoring finite horizon productions. *International Journal of Production Research*.

Chowdhury, S., Mukherjee, A., & Chakraborti, S. (2015). Distribution-free Phase II CUSUM control chart for joint monitoring of location and scale. *Quality and Reliability Engineering International*.

Conover, W. J., Guerrero-Serrano, A. J., & Tercero-Gómez, V. G. (2018). An update on a comparative study of tests for homogeneity of variance. *Journal of Statistical Computation and Simulation*.

Faria Sobue, C. E., Jardim, F. S., Camargo, V. C. B., Lizarelli, F. L., & Oprime, P. C. (2020). Unconditional performance of the xâc̄hart: Comparison among five standard deviation estimators. *Quality and Reliability Engineering International*.

Hollander, M., Wolfe, D., & Chicken, E. (2013). *Nonparametric Statistical Methods* (3rd ed.). Wiley.

Jardim, F. S., Chakraborti, S., & Epprecht, E. K. (2020). Two perspectives for designing a phase II control chart with estimated parameters: The case of the Shewhart $\bar{X}$ Chart. *Journal of Quality Technology*.

Jensen, W. A., Jones-Farmer, L. A., Champ, C. W., & Woodall, W. H. (2006). Effects of parameter estimation on control chart properties: A literature review. *Journal of Quality Technology*.

Kiran, D. (2017). Chapter 16 Fundamentals of Statistics Part I (D. Kiran, Ed.). In D. Kiran (Ed.), *Total quality management*. "Butterworth-Heinemann".

Lepage, Y. (1971). A combination of wilcoxon's and ansari-bradley's statistics. *Biometrika*.

Montgomery, D. C. (2009). *Introduction to statistical quality control*.

Mukherjee, A., & Chakraborti, S. (2012). A distribution-free control chart for the joint monitoring of location and scale. *Quality and Reliability Engineering International*.

Mukherjee, A., & Marozzi, M. (2020). Nonparametric phase-ii control charts for monitoring high-dimensional processes with unknown parameters. *Journal of Quality Technology*, 1–21.

Nenes, G., Celano, G., & Castagliola, P. (2017). Economic and Statistical Design of Vp Control Charts for Finite-Horizon Processes. *IISE Transactions*.

Nenes, G., Celano, G., Castagliola, P., & Panagiotido, S. (2014). The variable sampling interval control chart for finite-horizon processes. *IIE Transactions*.

Nenes, G., & Tagaras, G. (2010). Evaluation of cusum charts for finite-horizon processes. *Communications in Statistics - Simulation and Computation*.

Page, E. S. (1954). Continuous inspection schemes. *Biometrika*, 100–115.

Psarakis, S., Vyniou, A. K., & Castagliola, P. (2014). Some recent developments on the effects of parameter estimation on control charts. *Quality and Reliability Engineering International*.

Qiu, P. (2014). *Introduction to statistical process control*.

Roberts, S. W. (1959). Control chart tests based on geometric moving averages. *Technometrics*, 239–250.

Shewhart, W. A. (1926). Quality control charts. *The Bell System Technical Journal*, 593–603.

Tercero-Gómez, V., Aguilar-Lleyda, V., Cordero-Franco, A., & Conover, W. (2020). A distribution-free cusum chart for joint monitoring of location and scale based on the

combination of wilcoxon and mood statistics. *Quality and Reliability Engineering International*.

Zhang, P. (2010). Chapter 2 - industrial control engineering (P. Zhang, Ed.). In P. Zhang (Ed.), *Advanced industrial control technology*. William Andrew Publishing.

List of Figures

List of Tables